

CONTOUR INTEGRATION FOR EIGENVECTOR NONLINEARITIES*

ROB CLAES[†], KARL MEERBERGEN[‡], AND SIMON TELEN[§]

Abstract. Solving polynomial eigenvalue problems with eigenvector nonlinearities (PEPv) is an interesting computational challenge, outside the reach of the well-developed methods for nonlinear eigenvalue problems. We present a natural generalization of these methods which leads to a contour integration approach for computing all eigenvalues of a PEPv in a compact region of the complex plane. Our methods can be used to solve any suitably generic system of polynomial or rational function equations.

Key words. eigenvector nonlinearities, contour integration, polynomial equations, trace, polynomial eigenvalue problem

MSC codes. 65F15, 65H17, 65H04, 13P15

DOI. 10.1137/22M1497985

1. Introduction. We consider a matrix valued function $T : \mathbb{C}^n \times \mathbb{C} \rightarrow \mathbb{C}^{n \times n}$, $(x, z) \mapsto T(x, z)$ such that, for any fixed $z \in \mathbb{C}$, T is given by homogeneous polynomials in x , and for any fixed x , T is given by polynomials in z . We assume, moreover, that all polynomials in the i th row of T are of the same degree d_i . If any of these degrees is positive, the function T defines a polynomial eigenvalue problem with eigenvector nonlinearities (PEPv), given by the equation

$$(1.1) \quad T(x, z) \cdot x = 0.$$

By homogeneity, these equations are well defined on $\mathbb{P}^{n-1} \times \mathbb{C}$, where \mathbb{P}^{n-1} is the $(n - 1)$ -dimensional complex projective space. Points $(x^*, z^*) \in \mathbb{P}^{n-1} \times \mathbb{C}$ such that $T(x^*, z^*) \cdot x^* = 0$ are called eigenpairs. For such an eigenpair, z^* is the eigenvalue, with corresponding eigenvector x^* . This paper is concerned with computing all eigenpairs (x^*, z^*) for which z^* lies in a compact domain $\Omega \subset \mathbb{C}$, whose Euclidean boundary is denoted by $\partial\Omega$.

Example 1.1 ($n = 3, d_1 = d_2 = d_3 = 1$). Consider the PEPv given by

$$T(x, z) \cdot x = \begin{pmatrix} x_1 + zx_2 & zx_2 + x_3 & x_1 - x_3 \\ x_1 + (1+z)x_2 & (1-z^2)x_2 - zx_3 & x_1 + x_3 \\ (1+z)x_1 + x_2 & x_2 - x_3 & zx_1 + (1-z)x_3 \end{pmatrix} \cdot \begin{pmatrix} x_1 \\ x_2 \\ x_3 \end{pmatrix} = \begin{pmatrix} 0 \\ 0 \\ 0 \end{pmatrix}.$$

For fixed $z \in \mathbb{C}$, the entries of $T(x, z) \cdot x$ define three conics in \mathbb{P}^2 , given by $f_i(x, z) = 0$, $i = 1, 2, 3$. For instance, the equation of the first conic is $f_1 = x_1^2 + zx_1x_2 + zx_2^2 +$

*Received by the editors May 25, 2022; accepted for publication (in revised form) May 25, 2023; published electronically October 30, 2023.

<https://doi.org/10.1137/22M1497985>

Funding: The work of the first and second authors was supported by the Research Foundation Flanders (FWO) grant G0B7818N and the KU Leuven Research Council. The work of the third author was supported by a Veni grant from the Netherlands Organisation for Scientific Research (NWO).

[†]Computer Science, KU Leuven, Heverlee (Leuven) 3001, Belgium (rob.claes@kuleuven.be).

[‡]Computer Science, KU Leuven, Leuven, 3001, Belgium (Karl.Meerbergen@kuleuven.be).

[§]MPI-MiS Leipzig, 04103 Leipzig, Germany, and CWI Amsterdam, 1098 XG Amsterdam, Netherlands (simon.telen@mis.mpg.de).

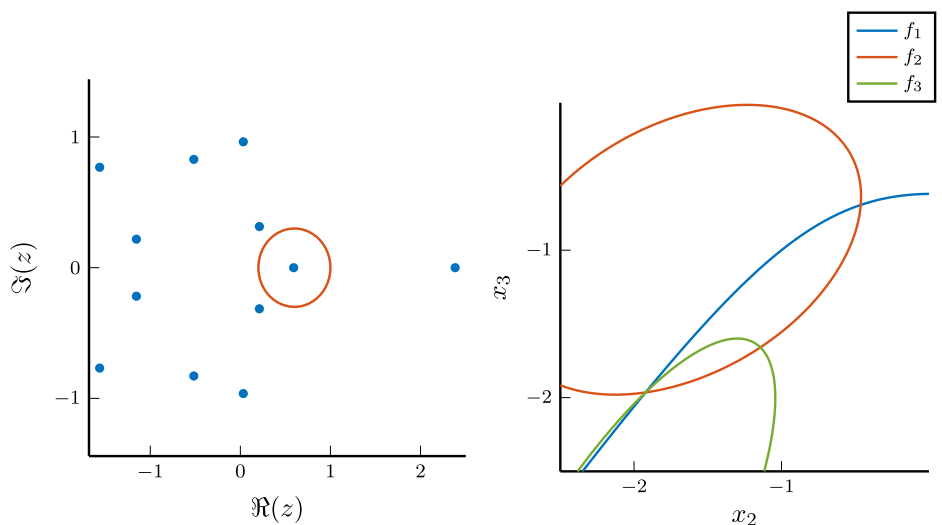
$x_2x_3 + x_1x_3 - x_3^2 = 0$. For fixed z , this is a homogeneous quadratic equation in the coordinates x on \mathbb{P}^2 . Usually, three conics have no common intersection points. The eigenvalues $z = z^*$ are precisely those choices of z for which the three conics intersect. The 12 eigenvalues are the roots of

$$\mathcal{R}(z) = 4z^{12} + 12z^{11} - z^{10} - 53z^9 - 100z^8 - 108z^7 - 78z^6 - 23z^5 + 14z^4 + 22z^3 + 8z^2 - 4z + 3,$$

depicted in Figure 1.1a. This polynomial is computed via resultants which will be explained in section 3. One of the eigenvalues is $z^* \approx 0.5919$, with eigenvector $x^* \approx (1 : -1.9218 : -1.9646) \in \mathbb{P}^2$. A possible choice for the target domain Ω to select this eigenvalue is shown in Figure 1.1a by its boundary $\partial\Omega$. The three conics corresponding to $z^* = 0.5919$ are shown in Figure 1.1b. More precisely, we plot the conics in the affine chart where $x_1 \neq 0$. For instance, the blue curve consists of all points (x_2, x_3) satisfying $f_1(1, x_2, x_3, z^*) = 0$.

Any system of polynomial equations $f_1(x, z) = \dots = f_n(x, z) = 0$ on $\mathbb{P}^{n-1} \times \mathbb{C}$ can be formulated as a PEPv. This leads to a wide variety of applications. An example is given in experiment 5 of section 7. Rewriting such a system as in (1.1) and calling solutions “eigenpairs” seemingly does not change much. Our motivation is that the algorithm we propose for finding eigenpairs with $z^* \in \Omega$ is a natural generalization of standard algorithms used for eigenvalue problems with more structure. More precisely, PEPv’s generalize polynomial eigenvalue problems (PEP) for which $d_i = 0$. These, in turn, contain generalized eigenvalue problems (GEP) for which $d_i = 0$ and $T(z) = A - z \cdot B$ is an affine-linear function.

Polynomial eigenvalue problems often arise from an intermediate step in solving general nonlinear eigenvalue problems (NEP), in which the entries of $T(z)$ are allowed to be transcendental functions of z . One typically approximates these functions by polynomials in a certain region of the complex plane, obtaining a PEP. One way of



(a) Eigenvalues (•) and contour $\partial\Omega$ (—). (b) Three conics corresponding to $z^* \approx 0.5919$.

FIG. 1.1. Example 1.1. (Figure in color online.)

solving PEPs is linearization [11, 24]. The linearization step results in a GEP of larger dimension. This dimension grows with the degree of the approximating polynomials, and is typically very large. In order to solve it, special structure exploiting methods are used [15, 23].

Another common approach for solving NEPs is based on contour integration. The goal of methods like Beyn [3], SS [1], or NLFEAST [13] is to locate all eigenvalues on a compact domain Ω in the complex plane. This is done by calculating a contour integral over the boundary $\partial\Omega$ with an integrand that contains the matrix inverse of the eigenvalue problem. Using the residue theorem, the poles of the integrand—which coincide with the desired eigenvalues in the compact domain—can be extracted.

In the present paper, we develop a new contour-integration-based method for finding all eigenpairs of a PEPv with $z^* \in \Omega$. It generalizes known approaches for PEPs in the sense that when $d_i = 0$, Beyn’s algorithm is recovered. We reiterate that, under suitable genericity assumptions, this can be used to find all solutions to a polynomial system $f_1(x, z) = \dots = f_n(x, z) = 0$ with z -coordinate inside Ω . The situation of interest is where the number of solutions with this property is much smaller than the total number of solutions, i.e., the total number of eigenvalues of $T(x, z)$. Our strategy is to integrate trace functions along the boundary $\partial\Omega$, and extract the eigenvalues from moments. These traces are evaluated using numerical homotopy continuation [17]. Such methods can also be used to naively compute all eigenpairs of $T(x, z)$ and then filter out relevant solutions by checking whether $z \in \Omega$. However, an important feature of our method is that evaluating the trace may require significantly less homotopy paths than the total number of eigenvalues of $T(x, z)$, which makes it more efficient than the naive approach (section 6). It is important to note that the traces are not available in an explicit form as is usually expected for PEPs solved by Krylov methods. Therefore, we only consider contour integration methods in this paper: these only require evaluation of the trace, not its explicit expression.

This paper is structured as follows. An overview of the standard Beyn’s algorithm is presented in section 2. The basis of our approach is laid in section 3 by introducing the concepts of resultants and traces. Section 4 relates the denominator of the trace to the resultant, and hence its poles to the eigenvalues. Section 5 describes the resulting contour integration method and comments on the numerical implementation. We discuss the complexity of our method in section 6 and present an analysis for two families of systems of equations. Our numerical experiments in section 7 confirm the presented theory, the Julia code used for these experiments is available online at github.com/robclaes/contour-integration.

2. Beyn’s algorithm. The method of Beyn [3] considers the nonlinear eigenvalue problem defined by the holomorphic matrix valued function $A : \mathbb{C} \rightarrow \mathbb{C}^{n \times n}$ as

$$A(z) \cdot x = 0.$$

The goal is to find eigenpairs $(x^*, z^*) \in \mathbb{P}^{n-1} \times \mathbb{C}$ for which the eigenvalue z^* lies in the compact domain Ω of the complex plane. The function A is typically assumed to be holomorphic in a neighborhood of Ω . Beyn’s method is especially useful for targeting a specific subset of the, possibly infinite, complete set of eigenvalues. In this section, we recapitulate the idea and theory behind contour integration for eigenvalue problems. For reasons of clarity, we focus the derivations on simple eigenvalues only. An eigenvalue is called simple if the algebraic multiplicity and the geometric multiplicity

are equal to one, where the multiplicity of an eigenvalue is defined by the following definitions.

DEFINITION 2.1. *The algebraic multiplicity of an eigenvalue z^* is the smallest positive integer m_a such that*

$$(2.1) \quad \frac{d^{m_a}}{dz^{m_a}} \det(A(z)) \Big|_{z=z^*} \neq 0.$$

DEFINITION 2.2. *The geometric multiplicity of an eigenvalue z^* is the dimension of the null space of $A(z^*)$.*

Let z^* be a simple eigenvalue of A with corresponding right and left eigenvectors x^* and y^* such that $A(z^*) \cdot x^* = 0$ and $A(z^*)^H \cdot y^* = 0$. Here $A(z^*)^H$ denotes Hermitian transpose of $A(z^*)$. There exists a region $\mathcal{N} \subset \mathbb{C}$ around z^* and a holomorphic function $R: \mathbb{C} \rightarrow \mathbb{C}^{n \times n}$ such that

$$A(z)^{-1} = \frac{1}{z - z^*} x^* y^{*H} + R(z), \quad z \in \mathcal{N} \setminus \{z^*\}.$$

This property can be easily generalized to the case where multiple simple eigenvalues are considered in a compact subset of \mathbb{C} [3, Thm. 2.4].

THEOREM 2.3. *Let $\Omega \subset \mathbb{C}$ be a compact subset that contains only the simple eigenvalues $z_i^*, i = 1, \dots, l$ with corresponding right and left eigenvectors x_i^* and y_i^* . Then there exists a neighborhood \mathcal{N} of Ω and a holomorphic function $R: \mathbb{C} \rightarrow \mathbb{C}^{n \times n}$ such that*

$$A(z)^{-1} = \sum_{i=1}^l \frac{1}{z - z_i^*} x_i^* y_i^{*H} + R(z), \quad z \in \mathcal{N} \setminus \{z_1^*, \dots, z_l^*\}.$$

Theorem 2.3 provides us with a way of expressing the value of a contour integral over the boundary of the compact subset $\Omega \subset \mathcal{N}$.

THEOREM 2.4. *In the situation of Theorem 2.3, we have that*

$$\frac{1}{2\pi\sqrt{-1}} \oint_{\partial\Omega} f(z) A(z)^{-1} dz = \sum_{i=1}^l f(z_i^*) x_i y_i^H.$$

Under the assumption that only a few eigenvalues lie within Ω , i.e., $l < n$, and all eigenvectors are linearly independent, we can extract the eigenvalues and corresponding eigenvectors from the following two contour integrals:

$$A_0 = \frac{1}{2\pi\sqrt{-1}} \oint_{\partial\Omega} A(z)^{-1} \hat{V} dz, \quad A_1 = \frac{1}{2\pi\sqrt{-1}} \oint_{\partial\Omega} z A(z)^{-1} \hat{V} dz,$$

with $\hat{V} \in \mathbb{C}^{n \times q}$, $q \geq l$ a random matrix of full rank q . Using Theorem 2.4, we see that

$$A_0 = \sum_{i=1}^l x_i^* y_i^{*H} \hat{V} = X Y^H \hat{V}, \quad A_1 = \sum_{i=1}^l z_i^* x_i^* y_i^{*H} \hat{V} = X Z Y^H \hat{V},$$

where X and Y have the right and left eigenvectors for their columns and Z is a diagonal matrix containing the corresponding eigenvalues. The matrix A_0 has rank at most l for random choices of \hat{V} , so that a reduced singular value decomposition can be expressed as

$$A_0 = V_0 \Sigma_0 W_0^H$$

with rectangular $V_0 \in \mathbb{C}^{n \times l}$ and $W_0 \in \mathbb{C}^{q \times l}$ and diagonal matrix $\Sigma_0 = \text{diag}(\sigma_1, \dots, \sigma_l)$. In [3] it is shown, via some linear algebra manipulations, that

$$V_0^H A_1 W_0 \Sigma_0^{-1} = SZS^{-1}.$$

This decomposition reveals the diagonal matrix Z containing the eigenvalues, while the corresponding eigenvectors can be extracted from $V = V_0 S$.

Since nonlinear eigenvalue problems can have more eigenvalues than the size of the matrix, it is necessary to extend this approach to the case where $l > n$. Luckily, Beyn’s algorithm generalizes easily to this case. First, the matrix $\hat{V} \in \mathbb{C}^{n \times n}$ is now a square matrix of full rank which is used to calculate so-called higher order moments of the contour integrals:

$$A_k = \frac{1}{2\pi\sqrt{-1}} \oint_{\partial\Omega} z^k A(z)^{-1} \hat{V} dz.$$

It should be clear that A_k can be decomposed as $A_k = XZ^k Y^H \hat{V}$. From these higher order moments, we can calculate two block Hankel matrices

$$(2.2) \quad B_0 = \begin{pmatrix} A_0 & \cdots & A_{M-1} \\ \vdots & & \vdots \\ A_{M-1} & \cdots & A_{2M-2} \end{pmatrix} \quad \text{and} \quad B_1 = \begin{pmatrix} A_1 & \cdots & A_M \\ \vdots & & \vdots \\ A_M & \cdots & A_{2M-1} \end{pmatrix}.$$

In a similar way as with few eigenvalues, it can be shown that the rank of B_0 is equal to the number of eigenvalues in Ω such that the diagonalizable matrix

$$V_0^H B_1 W_0 \Sigma_0^{-1} = SZS^{-1}$$

is defined by the reduced singular value decomposition $B_0 = V_0 \Sigma_0 W_0^H$. The eigenvalues are again the elements of the diagonal matrix Z while the corresponding eigenvectors can be extracted from $V_0^{[1]} S$ with $V_0^{[1]}$ the first n rows of V_0 . Some additional technicalities need to be considered in the case of semisimple and defective eigenvalues [3], but this falls outside the scope of this discussion.

We conclude this section with a discussion on how the moment matrices A_k are computed in practice. We assume that $\partial\Omega$ is parameterized by a continuous function $\varphi : [0, 2\pi) \rightarrow \mathbb{C}$. The moment matrix A_k is then expressed as

$$A_k = \frac{1}{2\pi\sqrt{-1}} \int_0^{2\pi} \varphi^k(t) A(\varphi(t))^{-1} \hat{V} \varphi'(t) dt.$$

This integral can be approximated numerically by the trapezoidal rule with N equidistant points $t_\ell = \frac{2\ell\pi}{N}, \ell = 0, \dots, N - 1$, as

$$A_k \approx A_{k,N} = \frac{1}{N\sqrt{-1}} \sum_{\ell=0}^{N-1} \varphi^k(t_\ell) A(\varphi(t_\ell))^{-1} \hat{V} \varphi'(t_\ell).$$

The choice of the trapezoidal rule integration scheme with equidistant points might feel somewhat arbitrary, but it often leads to satisfactory results with a limited amount of points [3]. The impact of the integration scheme on the accuracy of the results is discussed in [22].

The largest part of the computational cost of Beyn’s method originates from the calculation of the moment matrices. Note that most of the computation work can be reused between every moment matrix since the factor $A(\varphi(t_\ell))^{-1} \hat{V}$ is independent of the moment index k . Each linear system $A(\varphi(t_\ell))^{-1} \hat{V}$ can be solved independently for every value of t_ℓ which leads to an efficient parallel implementation. In what follows, our aim is to generalize Beyn’s method to the case with eigenvector nonlinearities.

Downloaded 11/29/23 to 192.16.191.136 . Redistribution subject to SIAM license or copyright; see https://pubs.siam.org/terms-privacy

3. Resultants and traces. In this section, we turn back to the PEPv from the introduction. We discuss resultants and traces related to our equations $T(x, z) \cdot x = 0$. We work in the ring $K[x] = K[x_1, \dots, x_n]$ of polynomials in the variables x_i with coefficients in the rational function field $K = \mathbb{C}(z)$. The polynomials $f_1, \dots, f_n \in K[x]$ are the entries of the vector $T(x, z) \cdot x$. We assume that f_i is homogeneous of degree $d_i + 1$ and write $f_i \in K[x_i]_{d_i+1}$.

For fixed values $z = z^*$, the system of polynomial equations $f_1 = \dots = f_n = 0$ encoded by the PEPv $T(x, z^*) \cdot x = 0$ consists of n homogeneous equations on \mathbb{P}^{n-1} . Generically, one expects such equations to have no solution with nonzero coordinates. The eigenvalues are those special values of z^* for which they *do* have solutions; see Example 1.1. This is captured by a polynomial $\mathcal{R}(z)$ obtained via *resultants*. We summarize the basics, and refer the reader to [6, Chapters 3 and 7] for more details. Let $\mathcal{A}_i \subset \mathbb{N}^n, i = 1, \dots, n$ denote the *supports* of the polynomials $f_i \in K[x]$: if $f_i = \sum_{\alpha \in \mathbb{N}^n} c_{i,\alpha}(z) x^\alpha$, where x^α is short for $x_1^{\alpha_1} \dots x_n^{\alpha_n}$, then

$$\mathcal{A}_i = \{\alpha \in \mathbb{N}^n \mid c_{i,\alpha} \neq 0\}.$$

We write $K[x]_{d_i+1} \supset K[x]_{\mathcal{A}_i} \simeq K^{|\mathcal{A}_i|}$ for the affine space of polynomials with coefficients in K and support contained in \mathcal{A}_i . A natural set of coordinates for $K[x]_{\mathcal{A}_i}$ is given by the coefficients $\{b_{i,\alpha} \mid \alpha \in \mathcal{A}_i\}$ of a generic polynomial with support \mathcal{A}_i . That is, a polynomial $h_i = \sum_{\alpha \in \mathcal{A}_i} b_{i,\alpha} x^\alpha \in K[x]_{\mathcal{A}_i}$ is represented by the point $(b_{i,\alpha})_{\alpha \in \mathcal{A}_i} \in K^{|\mathcal{A}_i|}$.

Let $Z_0 \subset K[x]_{\mathcal{A}_1} \times \dots \times K[x]_{\mathcal{A}_n}$ be the set of tuples (h_1, \dots, h_n) for which $h_1 = \dots = h_n = 0$ has a solution in $(K \setminus \{0\})^n$. This is, in general, not a variety. Its *Zariski closure* Z is the smallest algebraic variety containing Z_0 . That is,

$$Z = \overline{Z_0} \subset K[x]_{\mathcal{A}_1} \times \dots \times K[x]_{\mathcal{A}_n}.$$

Under mild assumptions on the \mathcal{A}_i , Z has codimension one, so that it is defined by one polynomial equation in the coefficients of h_1, \dots, h_n [18, Cor. 1.1], called the *sparse resultant*. This polynomial is denoted by $R_{\mathcal{A}_1, \dots, \mathcal{A}_n}$. It has integer coefficients, and it is irreducible over \mathbb{C} [18, Lem. 1.1]. In summary, the sparse resultant $R_{\mathcal{A}_1, \dots, \mathcal{A}_n}$ is the unique (up to sign) irreducible polynomial in $\mathbb{Z}[b_{i,\alpha} \mid i = 1, \dots, n, \alpha \in \mathcal{A}_i]$ such that

$$(h_1, \dots, h_n) \in Z \iff R_{\mathcal{A}_1, \dots, \mathcal{A}_n}(h_1, \dots, h_n) = 0.$$

Example 3.1. Let $\mathcal{A}_i = \{(1, 0, \dots, 0), (0, 1, \dots, 0), \dots, (0, 0, \dots, 1)\}$ consist of the list of standard basis vectors for $i = 1, \dots, n$. The polynomials h_i are generic linear forms in x_1, \dots, x_n :

$$\begin{pmatrix} h_1 \\ h_2 \\ \vdots \\ h_n \end{pmatrix} = \begin{pmatrix} b_{11} & b_{12} & \dots & b_{1n} \\ b_{21} & b_{22} & \dots & b_{2n} \\ \vdots & \vdots & & \vdots \\ b_{n1} & b_{n2} & \dots & b_{nn} \end{pmatrix} \cdot \begin{pmatrix} x_1 \\ x_2 \\ \vdots \\ x_n \end{pmatrix} = B \cdot x.$$

Since there is a nonzero solution to $h_1 = \dots = h_n = 0$ if and only if B is singular, we have $R_{\mathcal{A}_1, \dots, \mathcal{A}_n} = \det B$. The resultant is a homogeneous polynomial of degree n in n^2 variables.

Example 3.2. Let $n = 2$ and $\mathcal{A}_i = \{(2, 0), (1, 1), (0, 2)\}$ for $i = 1, 2$. In this case we are asking for which coefficients $b_{11}, b_{12}, b_{13}, b_{21}, b_{22}, b_{23}$ the two binary quadrics

$$h_1 = b_{11}x_1^2 + b_{12}x_1x_2 + b_{13}x_2^2 \quad \text{and} \quad h_2 = b_{21}x_1^2 + b_{22}x_1x_2 + b_{23}x_2^2$$

have a common root in \mathbb{P}^1 . Sylvester’s formula [6, Chapter 3, sect. 1] writes the resultant as

$$R_{\mathcal{A}_1, \mathcal{A}_2} = \det \begin{pmatrix} b_{11} & 0 & b_{21} & 0 \\ b_{12} & b_{11} & b_{22} & b_{21} \\ b_{13} & b_{12} & b_{23} & b_{22} \\ 0 & b_{13} & 0 & b_{23} \end{pmatrix}.$$

This is a homogeneous degree 4 polynomial in our six variables with integer coefficients.

Example 3.3. Let $\mathcal{A} = \mathcal{A}_1 = \mathcal{A}_2 = \mathcal{A}_3 \subset \mathbb{Z}^3$ consist of all monomials of degree 2 in three variables. Consider 3 general ternary quadrics

$$h_i = b_{i,1}x_1^2 + b_{i,2}x_2^2 + b_{i,3}x_3^2 + b_{i,4}x_1x_2 + b_{i,5}x_1x_3 + b_{i,6}x_2x_3, \quad i = 1, 2, 3.$$

The resultant $R_{\mathcal{A}, \mathcal{A}, \mathcal{A}}$ is a polynomial of degree 12 in the 18 variables $b_{i,j}$, $i = 1, \dots, 3$, $j = 1, \dots, 6$, which characterizes when the three conics $\{h_i = 0\} \subset \mathbb{P}^2$ intersect. It has 21894 terms and can be computed as a 6×6 determinant; see [6, Chapter 3, sect. 2].

Evaluating the sparse resultant $R_{\mathcal{A}_1, \dots, \mathcal{A}_n}$ at our tuple $(f_1, \dots, f_n) \in K[x]^n$ means plugging in the coefficients $c_{i,\alpha}(z) \in K$ for the $b_{i,\alpha}$. Since we assume the coefficients of the f_i to be polynomials in z , we obtain a polynomial

$$(3.1) \quad \mathcal{R}(z) = R_{\mathcal{A}_1, \dots, \mathcal{A}_n}(f_1, \dots, f_n) \in \mathbb{C}[z].$$

The zeros of $\mathcal{R}(z)$ capture the values of z for which $f_1 = \dots = f_n = 0$ has a solution.

Example 3.4. In the case of a EP given by $T(z) \cdot x = 0$, we have $\mathcal{R}(z) = \det T(z)$. This is obtained by substituting the entries of $T(z)$ into the matrix B from Example 3.1.

Example 3.5. Plugging in the coefficients of the polynomials f_1, f_2, f_3 in Example 1.1 into the 6×6 determinant from Example 3.3, i.e., $b_{1,1} = 1, b_{1,2} = z, b_{1,3} = -1, b_{1,4} = z, \dots$, we obtain the degree 12 polynomial $\mathcal{R}(z) = R_{\mathcal{A}, \mathcal{A}, \mathcal{A}}(f_1, f_2, f_3)$ shown in Example 1.1.

As illustrated by Example 3.5, the roots of the polynomial $\mathcal{R}(z)$ are eigenvalues of the PEPv given by $T(x, z) \cdot x = 0$. We propose the following notion of *regularity* for a PEPv.

DEFINITION 3.1. *The PEPv given by $T(x, z) \cdot x = 0$ is called regular if $\mathcal{R}(z) \neq 0$.*

By Example 3.4, this agrees with the definition of regularity for PEPs. Unlike for PEPs, regularity of a PEPv does not mean that there are finitely many eigenvalues.

Example 3.6. We consider the PEPv $T(x, z) \cdot x = 0$ where

$$T(x, z) = \begin{pmatrix} x_1 & (1+z)x_1 & x_2 \\ 2x_1 & 3x_1 & (3+z)x_2 \\ 2zx_1 & x_1 & x_2 \end{pmatrix} \quad \text{and} \quad \begin{aligned} f_1 &= x_1^2 + (1+z)x_1x_2 + x_2x_3, \\ f_2 &= 2x_1^2 + 3x_1x_2 + (3+z)x_2x_3, \\ f_3 &= 2zx_1^2 + x_1x_2 + x_2x_3. \end{aligned}$$

We calculate $\mathcal{R}(z) = 2z^3 + 8z^2 - 3z \neq 0$. However, for any $z^* \in \mathbb{C}$, we have that $T(x^*, z^*) \cdot x^* = 0$, with $x^* = (0, 0, 1)^\top$ or $x^* = (0, 1, 0)^\top$.

To avoid such artefacts, we will limit ourselves to computing eigenpairs (z^*, x^*) for which x^* has no zero coordinates. That is, we look for eigenvectors in the *algebraic*

torus $\{x \in \mathbb{P}^{n-1} \mid x_i \neq 0, i = 1, \dots, n\}$. For such an eigenpair, we say that z^* is an *eigenvalue with toric eigenvector*. By the definition of the resultant, if $z^* \in \mathbb{C}$ is an eigenvalue of $T(x, z)$ with toric eigenvector, then $\mathcal{R}(z^*) = 0$. This implies the following statement.

THEOREM 3.2. *A regular PEPv has finitely many eigenvalues with toric eigenvector.*

It is *not* true, in general, that each z^* such that $\mathcal{R}(z^*) = 0$ is an eigenvalue with toric eigenvector. We continue Example 3.6.

Example 3.7. There are no toric solutions to $T(x, z^*) \cdot x = 0$, with $z^* = 0$ and T as in Example 3.6. For readers familiar with toric geometry, we point out that this eigenvalue appears in $\mathcal{R}(z)$ because it corresponds to a solution of $T(x, z^*) \cdot x = 0$ in a toric compactification of $(\mathbb{C} \setminus \{0\})^n$. For this eigenvalue, there is an “extra” nontoric eigenvector $(0, 1, -1)^\top$.

DEFINITION 3.3. *An eigenvalue of the PEPv $T(x, z) \cdot x = 0$ with toric eigenvector is called simple if it is a simple zero of $\mathcal{R}(z)$.*

Example 3.8. In Example 1.1, $z^* \approx 0.5919$ is a simple eigenvalue with toric eigenvector.

It is usually hard to compute $\mathcal{R}(z)$. We now turn to *traces*, which are rational functions in z whose denominator is $\mathcal{R}(z)$. The upshot is that these traces can be evaluated using tools from numerical nonlinear algebra. Once we know how to evaluate, we can approximate residue integrals to compute the poles of the trace. Since the denominator is $\mathcal{R}(z)$, these poles are our eigenvalues.

We fix n random homogeneous polynomials $a_1, \dots, a_n \in \mathbb{C}[x]$ such that $\deg(a_i) = d_i = \deg(f_i) - 1$. We write $a_i \in \mathbb{C}[x]_{d_i}$ and collect them in a vector $a = (a_1, \dots, a_n)^\top \in \mathbb{C}[x]^n$. Consider the ideal I_a generated by the entries of $T(x, z) \cdot x - a$:

$$(3.2) \quad I_a = \langle f_1 - a_1, \dots, f_n - a_n \rangle \subset K[x, x^{-1}].$$

Here $K[x, x^{-1}] = K[x_1^{\pm 1}, \dots, x_n^{\pm 1}]$ is the Laurent polynomial ring in n variables with coefficients in K . Note that the ideal I_a is *not* homogeneous. We will assume throughout that the equations $f_i - a_i = 0$ have finitely many solutions in $(\overline{K} \setminus \{0\})^n$, where \overline{K} is the algebraic closure of K . This is the field of Puiseux series $\overline{K} = \mathbb{C}\{\{z\}\}$. By [7, Chapter 5, sect. 3, Theorem 6], our assumption can equivalently be phrased as follows.

Assumption 1. The dimension $\delta = \dim_K K[x, x^{-1}]/I_a$ is finite.

This is a natural assumption, since I_a is generated by n (nonhomogeneous) equations in n unknowns. The set of solutions to $f_1 - a_1 = \dots = f_n - a_n = 0$ is denoted by

$$(3.3) \quad V(I_a) = \{\xi \in (\overline{K} \setminus \{0\})^n \mid f_i(\xi) - a_i(\xi) = 0, i = 1, \dots, n\}.$$

A point $\xi \in V(I_a)$ has multiplicity $\mu(\xi)$. By Assumption 1, $\sum_{\xi \in V(I_a)} \mu(\xi) = \delta$.

DEFINITION 3.4. *For a polynomial $p \in K[x, x^{-1}]$, the trace $\text{Tr}_p(I_a)$ is $\sum_{\xi \in V(I_a)} \mu(\xi) p(\xi)$.*

Remark 3.1. In linear algebra, the trace $\text{tr}(A)$ of a matrix A is the sum of its eigenvalues. Hence, it equals the sum of the values of the polynomial $p = x$ at the

nonzero roots of $\chi(x) = \det(x \cdot \text{id} - A)$ where we used “id” to indicate the identity operator. In symbols, we have $\text{tr}(A) = \text{Tr}_x(\langle \chi(x) \rangle)$.

PROPOSITION 3.5. *For any Laurent polynomial $p \in K[x, x^{-1}]$, the trace $\text{Tr}_p(I_a)$ is a rational function in z . That is, $\text{Tr}_p(I_a) \in K$.*

Proof. This is a standard result from Galois theory; see, for instance, [16, Chapter 6, Thm. 1.2]. Another way to see this explicitly is by considering the K -linear map

$$M_p : K[x, x^{-1}]/I_a \longrightarrow K[x, x^{-1}]/I_a \quad \text{given by} \quad [f] \longmapsto [pf],$$

where $[f]$ denotes the residue class of $f \in K[x, x^{-1}]$ in $K[x, x^{-1}]/I_a$. This is called a *multiplication map*. A matrix representation of such a map can be computed using linear algebra over K . A standard algorithm uses Gröbner bases [6, Chapter 2, sect. 4]. Since M_p can be represented by a $\delta \times \delta$ matrix with entries in K , its trace $\text{tr}(M_p)$ lies manifestly in K . Moreover, since the trace is the sum of the eigenvalues, [6, Chapter 4, sect. 2, Prop. 2.7] gives $\text{tr}(M_p) = \text{Tr}_p(I_a)$. \square

Example 3.9. Let T be as in Example 1.1. The number δ is the number of Puiseux series solutions $x(z) = (x_1(z), x_2(z), x_3(z))$ to $f_1 - a_1 = f_2 - a_2 = f_3 - a_3 = 0$, with

$$\begin{aligned} f_1 - a_1 &= x_1^2 + zx_1x_2 + zx_2^2 + x_2x_3 + x_1x_3 - x_3^2 - (b_{11}x_1 + b_{12}x_2 + b_{13}x_3), \\ f_2 - a_2 &= x_1^2 + (1+z)x_1x_2 + (1-z^2)x_2^2 - zx_2x_3 + x_1x_3 + x_3^2 - (b_{21}x_1 + b_{22}x_2 + b_{23}x_3), \\ f_3 - a_3 &= (1+z)x_1^2 + x_1x_2 + x_2^2 - x_2x_3 + zx_1x_3 + (1-z)x_3^2 - (b_{31}x_1 + b_{32}x_2 + b_{33}x_3). \end{aligned}$$

Here $a_i = b_{i1}x_1 + b_{i2}x_2 + b_{i3}x_3$ are generic linear forms. Using **Maple**, we find $\delta = 8$ and

$$\text{Tr}_{x_2}(I_a) = \frac{(16b_{11} + 8b_{13})z^{11} + (-4b_{33} + \dots - 16b_{31})z^{10} + \dots + (-8b_{33} + \dots + 2b_{32})}{\mathcal{R}(z)},$$

where $\mathcal{R}(z)$ is the polynomial from Example 1.1.

The fact that $\mathcal{R}(z)$ shows up as the denominator of $\text{Tr}_{x_2}(I_a)$ in Example 3.9 is no coincidence. The fact that this happens generally is the main result of the next section.

4. From traces to eigenvalues. This section relates the algebraic objects $\mathcal{R}(z)$ and $\text{Tr}_p(I_a)$ defined in section 3. The main result (Theorem 4.1) leads to our strategy for solving a PEPv. In short, the reasoning is as follows:

- (1) The roots of the polynomial $\mathcal{R}(z)$ are the eigenvalues of $T(x, z)$.
- (2) The trace $\text{Tr}_p(I_a)$ is a rational function in z whose denominator is (roughly) $\mathcal{R}(z)$.
- (3) Traces can be evaluated using tools from numerical nonlinear algebra. This allows one to perform numerical *contour integration* along $\partial\Omega$ to compute eigenvalues.

Point (1) was motivated in section 3. This section deals with (2), and (3) is the subject of the next section.

Recall that our PEPv defines n homogeneous polynomials f_i of degree $d_i + 1$, and the ideal I_a is generated by $f_i - a_i$, where $a_i \in \mathbb{C}[x]_{d_i}$. As in section 3, we write $\mathcal{A}_i \subset \mathbb{Z}^n$ for the monomial support of f_i . Similarly, the supports of the polynomials a_i are denoted \mathcal{B}_i , $i = 1, \dots, n$. We set $\mathcal{A}_0 = \{e_1, \dots, e_n\}$ with e_i the i th standard basis vector of \mathbb{Z}^n , $\mathcal{B}_0 = \{0\}$, and $\mathcal{C}_i = \mathcal{A}_i \cup \mathcal{B}_i$ for $i = 0, \dots, n$. The set $\mathcal{C}_0 = \{0\} \cup \mathcal{A}_0$ contains all lattice points of the standard simplex in \mathbb{Z}^n . The resultant $R_{\mathcal{C}_0, \mathcal{C}_1, \dots, \mathcal{C}_n}$ is

a polynomial in $b_{i,\gamma}, i = 0, \dots, n, \gamma \in \mathcal{C}_i$, characterizing when $h_0 = \dots = h_n = 0$ has a solution in $(\mathbb{C} \setminus \{0\})^n$, with $h_i = \sum_{\gamma \in \mathcal{C}_i} b_{i,\gamma} x^\gamma$.

Remark 4.1. Note that $R_{\mathcal{C}_0, \mathcal{C}_1, \dots, \mathcal{C}_n}$ is defined for $n+1$ polynomials h_0, \dots, h_n in n variables x_1, \dots, x_n , unlike in section 3, where the number of equations equals the number of variables. This is because the h_i are not homogeneous. To switch to the setting of section 3, one simply homogenizes the h_i . For instance, the resultant $R_{\mathcal{C}_1, \mathcal{C}_2}$ with $\mathcal{C}_1 = \mathcal{C}_2 = \{0, 1, 2\} \subset \mathbb{Z}^1$ vanishes when $b_{11}x^2 + b_{12}x + b_{13} = b_{21}x^2 + b_{22}x + b_{23} = 0$ has a solution. This is the same as $R_{\mathcal{A}_1, \mathcal{A}_2}$ from Example 3.2, where $\mathcal{A}_1 = \mathcal{A}_2$ is obtained by homogenizing the polynomials.

Our main result of this section makes point (2) above precise, under some assumptions (Assumptions 2 and 3) on the f_i and I_a that we will state below.

THEOREM 4.1. *Let $T(x, z) \cdot x = (f_1, \dots, f_n)^\top = 0$ be a PEPv satisfying Assumption 2, and let $a_i \in \mathbb{C}[x]_{d_i}$ be such that I_a satisfies Assumption 3. Let \mathcal{C}_i be the support of $f_i - a_i$ and $\mathcal{C}_0 = \{0, e_1, \dots, e_n\}$. The PEPv given by $T(x, z)$ is regular and for $p = \sum_{\gamma \in \mathcal{C}_0} c_{0,\gamma} x^\gamma$ we have*

$$(4.1) \quad \text{Tr}_p(I_a) = \frac{\mathcal{Q}_{p,a}(z)}{\mathcal{R}(z) \cdot \mathcal{S}_a(z)},$$

$$\text{where } \mathcal{Q}_{p,a}(z) = \sum_{\gamma \in \mathcal{C}_0} c_{0,\gamma} \frac{\partial R_{\mathcal{C}_0, \mathcal{C}_1, \dots, \mathcal{C}_n}}{\partial b_{0,\gamma}}(1, f_1 - a_1, \dots, f_n - a_n),$$

$\mathcal{R}(z)$ is as in (3.1) and $\mathcal{S}_a(z)$ is a nonzero polynomial.

Here *regularity* of $T(x, z)$ is in the sense of Definition 3.1. We wrote *roughly* in point (2) because the denominator may have a spurious factor $\mathcal{S}_a(z)$. This did not happen in Example 3.9, where $\mathcal{S}_a(z) = 1$. Here is an example where $\mathcal{S}_a(z)$ is not constant.

Example 4.1. Consider the PEPv $T(x, z) \cdot x = 0$ given by

$$T(x, z) = \begin{pmatrix} 1 & z & 1 \\ 2 & 1 & z \\ x_2 & (z+1)x_3 + x_2 & 0 \end{pmatrix}.$$

This satisfies Assumptions 2 and 3. We have $\mathcal{C}_0 = \{(0, 0, 0), (1, 0, 0), (0, 1, 0), (0, 0, 1)\}$, $a_1, a_2 \in \mathbb{C}$ and $a_3(x) = b_{31}x_1 + b_{32}x_2 + b_{33}x_3$. The trace for $p = x_1$ is

$$(4.2) \quad \text{Tr}_{x_1}(I_a) = \frac{b_{31}z^4 + (a_1 + a_2 - b_{32} - 2b_{33})z^3 + \dots + (2a_1 + 4a_2 + b_{31} - 2b_{32} - b_{33})}{(z^2 + 2z - 2)(z - 2)}.$$

Here $\mathcal{R}(z) = z^2 + 2z - 2$ and $\mathcal{S}_a(z) = z - 2$ is independent of a . We will explain the extraneous factor $\mathcal{S}_a(z)$ in Example A.1 below.

Before proving Theorem 4.1, we state Assumptions 2 and 3. The following example will help us to motivate Assumption 2.

Example 4.2. Let $f_1 = x_1^2 + x_2^2, f_2 = x_1^2 + zx_2^2$ and $a_1 = x_1, a_2 = x_2$. Summing the x_1 -coordinates of the solutions to $f_1 - a_1 = f_2 - a_2 = 0$, one computes that

$$\text{Tr}_{x_1}(I_a) = \frac{2z}{z-1}.$$

However, plugging the coefficients of f_1, f_2 into the resultant $R_{\mathcal{A}_1, \mathcal{A}_2}$ from Example 3.2, we obtain $\mathcal{R}(z) = (z - 1)^2$. The eigenvalue $z^* = 1$ is not simple. It has two toric eigenvectors: $(1, \sqrt{-1})^\top$ and $(-1, \sqrt{-1})^\top$. One can make this eigenvalue simple by applying a simple change of coordinates to the PEPv. We set $y_1 = x_1^2$ and $y_2 = x_2^2$ and obtain the new equations $\tilde{f}_1 = y_1 + y_2, \tilde{f}_2 = y_1 + zy_2$. The a_i now need to be replaced by constants. We set $\tilde{a}_1 = 1, \tilde{a}_2 = 1$. The trace of y_1 is the y_1 -coordinate of the unique solution:

$$\text{Tr}_{y_1}(I_{\tilde{a}}) = \frac{z - 2}{z - 1}.$$

The resultant polynomial is now $\tilde{\mathcal{R}}(z) = z - 1$ and coincides with the denominator, as desired. The eigenvalue $z^* = 1$ is now simple with eigenvector $(1, -1)$, and the original two eigenvectors can easily be recovered by undoing the coordinate change. Although the formula of Theorem 4.1 still holds in this example (the polynomial $\mathcal{Q}_{x_1, a}(z)$ also vanishes at $z = 1$), it is natural and convenient to assume that whenever such a coordinate change is possible, it is performed a priori. This is the essential content of Assumption 2 below.

To see whether a coordinate transformation like that in Example 4.2 is possible, one looks at the *lattice affinely generated by* $\mathcal{A}_1, \dots, \mathcal{A}_n$. This is the sublattice of \mathbb{Z}^n given by

$$L(\mathcal{A}_1, \dots, \mathcal{A}_n) = \left\{ \sum_{\alpha \in \mathcal{A}_1} \ell_{1, \alpha} \alpha + \dots + \sum_{\alpha \in \mathcal{A}_n} \ell_{n, \alpha} \alpha \mid \sum_{\alpha \in \mathcal{A}_i} \ell_{i, \alpha} = 0, \ell_{i, \alpha} \in \mathbb{Z} \right\}.$$

Since the polynomials f_i are homogeneous, we have $L(\mathcal{A}_1, \dots, \mathcal{A}_n) \subset \{\alpha \in \mathbb{Z}^n \mid \alpha_1 + \dots + \alpha_n = 0\}$. If this is a strict inclusion, a change of coordinates simplifies the PEPv.

Example 4.3. In Example 4.2, the supports are $\mathcal{A}_1 = \mathcal{A}_2 = \{(2, 0), (0, 2)\}$. These affinely generate a sublattice $L(\mathcal{A}_1, \mathcal{A}_2) \subsetneq \{\alpha \in \mathbb{Z}^2 \mid \alpha_1 + \alpha_2 = 0\}$, shown in the left part of Figure 4.1. After changing coordinates, the supports of \tilde{f}_1, \tilde{f}_2 are $\tilde{\mathcal{A}}_1 = \tilde{\mathcal{A}}_2 = \{(1, 0), (0, 1)\}$. The red lattice $L(\tilde{\mathcal{A}}_1, \tilde{\mathcal{A}}_2)$ now coincides with the full green lattice, see the right part of Figure 4.1.

Assumption 2. The lattice $L(\mathcal{A}_1, \dots, \mathcal{A}_n)$ is equal to $\{\alpha \in \mathbb{Z}^n \mid \alpha_1 + \dots + \alpha_n = 0\}$. This can always be realized by a change of coordinates as long as $L(\mathcal{A}_1, \dots, \mathcal{A}_n)$ has rank $n - 1$.

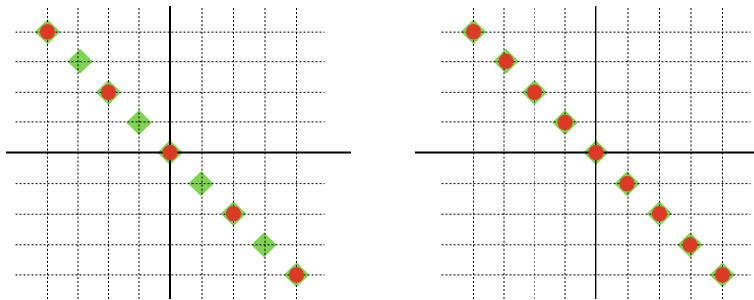


FIG. 4.1. The lattices $L(\mathcal{A}_1, \mathcal{A}_2)$ (left) and $L(\tilde{\mathcal{A}}_1, \tilde{\mathcal{A}}_2)$ (right) from Example 4.3 shown as red dots, and the lattice $\{\alpha \in \mathbb{Z}^2 \mid \alpha_1 + \alpha_2 = 0\}$ shown as green diamonds. (Figure in color online.)

Downloaded 11/29/23 to 192.16.191.136 . Redistribution subject to SIAM license or copyright; see https://epubs.siam.org/terms-privacy

This assumption is natural: if it is not satisfied the PEPv can be simplified. We leave the details of the general coordinate transformation as an easy exercise to the reader.

Our second assumption is that the equations $f_1 - a_1 = \dots = f_n - a_n = 0$ have the expected number of solutions in $(\overline{K} \setminus \{0\})^n$. To make this precise, we denote by $P_i = \text{Conv}(\mathcal{C}_i) \subset \mathbb{R}^n$ the *Newton polytope* of $f_i - a_i$. This is the convex hull of the lattice points in \mathcal{C}_i . The *mixed volume* of P_1, \dots, P_n , denoted $\text{MV}(P_1, \dots, P_n)$, is the generic number of solutions to a system of equations with supports $\mathcal{C}_1, \dots, \mathcal{C}_n$. For definitions and examples; see, for instance, [19, sect. 5.1] or [6, Chapter 7, sect. 5].

Assumption 3. The dimension $\delta = \dim_K K[x, x^{-1}]/I_a$ equals $\text{MV}(P_1, \dots, P_n)$. Equivalently, $V(I_a)$ from (3.3) consists of the expected number of points in $(\overline{K} \setminus \{0\})^n$.

This assumption is also quite mild, as the polynomials a_i can be chosen randomly. Having specified Assumptions 2 and 3, we are now ready to state the proof of Theorem 4.1.

Proof of Theorem 4.1. Our starting point is Theorem 2.3 in [8], which expresses the trace as

$$\text{Tr}_p(I_a) = C \cdot \frac{\mathcal{Q}_{p,a}(z)}{R_{\mathcal{C}_0, \dots, \mathcal{C}_n}(1, f_1 - a_1, \dots, f_n - a_n)}$$

for a nonzero constant C . Proposition 2.6 in the same paper writes the denominator $R_{\mathcal{C}_0, \dots, \mathcal{C}_n}(1, f_1 - a_1, \dots, f_n - a_n)$ as a product of *face resultants*. More precisely, adopting the standard notation used in [8] (which is recalled in Appendix A), we have

$$R_{\mathcal{C}_0, \dots, \mathcal{C}_n}(1, f_1 - a_1, \dots, f_n - a_n) = \prod_{\omega} R_{\mathcal{C}_1^{\omega}, \dots, \mathcal{C}_n^{\omega}}((f_1 - a_1)^{\omega}, \dots, (f_n - a_n)^{\omega})^{\delta_{\omega}},$$

where the product ranges over the primitive inward pointing facet normals ω of the Minkowski sum $P_1 + \dots + P_n$. The exponents δ_{ω} are defined combinatorially from the \mathcal{C}_i in the discussion preceding [8, Proposition 2.6]. By Assumption 3, none of the face resultants vanishes identically. Let $\omega^* = (-1, \dots, -1) \in (\mathbb{Z}^n)^{\vee}$. We have $\mathcal{C}_i^{\omega^*} = \mathcal{A}_i$ and $(f_i - a_i)^{\omega^*} = f_i$, which shows that $T(x, z)$ is regular and that $\mathcal{R}(z)^{\delta_{\omega^*}}$ is a factor in the denominator of $\text{Tr}_p(I_a)$. Assumption 2 and the fact that $\text{Conv}(\mathcal{C}_0)$ is a standard simplex imply $\delta_{\omega^*} = 1$. The theorem follows by setting $\mathcal{S}_a(z) = C^{-1} \cdot \prod_{\omega \neq \omega^*} R_{\mathcal{C}_1^{\omega}, \dots, \mathcal{C}_n^{\omega}}((f_1 - a_1)^{\omega}, \dots, (f_n - a_n)^{\omega})^{\delta_{\omega}}$. \square

Our main interest in Theorem 4.1 comes from the following immediate consequence.

COROLLARY 4.2. *If the PEPv $T(x, z) \cdot x = (f_1, \dots, f_n)^{\top} = 0$ and the ideal I_a satisfy Assumptions 2 and 3, then an eigenvalue z^* of $T(x, z)$ with toric eigenvector is a pole of $\text{Tr}_p(I_a)$ if $\mathcal{Q}_{p,a}(z^*) \neq 0$. Moreover, simple such eigenvalues correspond to simple poles of the trace.*

In the above notation. It would be desirable to have $\mathcal{S}_a(z)$ equal to a nonzero constant. In Appendix A, we identify two important families of PEPv for which this happens.

We conclude by briefly discussing the condition $\mathcal{Q}_{p,a}(z^*) \neq 0$. First, note that Assumption 3 implies $\text{Tr}_1(I_a) = \delta$, so by Theorem 4.1 we have

$$\mathcal{Q}_{1,a}(z) = \frac{\partial R_{\mathcal{C}_0, \dots, \mathcal{C}_n}}{\partial b_{0,0}}(1, f_1 - a_1, \dots, f_n - a_n) = \delta \mathcal{R}(z) \mathcal{S}_a(z).$$

In particular, $\mathcal{Q}_{1,a}(z^*) = 0$ for every eigenvalue z^* with toric eigenvector. Therefore, we will use the traces $\text{Tr}_{x_i}(I_a)$, corresponding to the remaining exponents $\mathcal{A}_0 = \mathcal{C}_0 \setminus \{0\}$.

DEFINITION 4.3. *We say that an eigenvalue z^* of $T(x, z)$ has a simple toric eigenvector if $\mathcal{R}(z^*) = 0$ and, for generic choices of a_i , there is some $i \in \{1, \dots, n\}$ for which $\mathcal{Q}_{x_i,a}(z^*) \neq 0$.*

We point out that if z^* has a simple toric eigenvector, then for generic a_i the tuple $(1, f_1(x, z^*) - a_1(x), \dots, f_n(x, z^*) - a_n(x))$ is a smooth point on the resultant hypersurface given by $\{R_{c_0, \dots, c_n} = 0\}$. This implies that the corresponding eigenvector is unique. We summarize the above discussion in the following theorem.

THEOREM 4.4. *Under Assumptions 2 and 3, each simple eigenvalue z^* of $T(x, z)$ with simple toric eigenvector is a pole of order one of the trace vector $(\text{Tr}_{x_1}(I_a), \dots, \text{Tr}_{x_n}(I_a)) \in \mathbb{C}(z)^n$. (In the situations of Theorems A.1 and A.2, all simple poles correspond to such eigenvalues.)*

We leave the problem of determining the precise conditions under which a simple eigenvalue has a simple toric eigenvector for future research. In our examples and experiments from section 7, we observe that this is satisfied for all simple eigenvalues.

5. Contour integration and homotopy continuation. Let $T(x, z)$ be a PEPv satisfying Assumptions 2 and 3. We write the trace vector from Theorem 4.4 as $\text{Tr}_{\mathcal{A}_0}(I_a) = (\text{Tr}_{x_1}(I_a), \dots, \text{Tr}_{x_n}(I_a))$. Using Definition 3.4 and Assumption 3, we see that the entries of $\text{Tr}_{\mathcal{A}_0}(I_a)$ are computed as a sum of $\delta = |V(I_a)|$ terms:

$$(5.1) \quad \text{Tr}_{x_i}(I_a) = \sum_{\xi \in V(I_a)} \xi_i.$$

The simple eigenvalues with simple toric eigenvector of $T(x, z)$ are among the poles of $\text{Tr}_{\mathcal{A}_0}(I_a)$. We remind the reader that $a \in \mathbb{C}[x]$ has homogeneous entries of degree d_i , where d_i is the degree in x of the entries in the i th row of $T(x, z)$. In analogy with Beyn’s method, we evaluate the trace for several vectors a . We collect $\text{Tr}_{\mathcal{A}_0}(I_{a^{(j)}})$ for n random choices $a^{(1)}, \dots, a^{(n)} \in \mathbb{C}^n$ in the columns of

$$(5.2) \quad U(z) = \begin{pmatrix} | & & | \\ \text{Tr}_{\mathcal{A}_0}(I_{a^{(1)}}) & \cdots & \text{Tr}_{\mathcal{A}_0}(I_{a^{(n)}}) \\ | & & | \end{pmatrix} \in \mathbb{C}(z)^{n \times n}.$$

Our next result uses notation from Theorem 4.1 and explains our interest in the matrix $U(z)$.

THEOREM 5.1. *Let $U(z)$ be as above, and let $Q(z) = (\mathcal{Q}_{x_i,a^{(j)}}(z))_{i,j}$. Suppose that $\det Q(z) \neq 0$ and z^* is a simple eigenvalue of $T(x, z)$ with simple toric eigenvector $x^* \in \mathbb{P}^{n-1}$. If $\mathcal{S}_{a^{(j)}}(z^*) \neq 0$ for $j = 1, \dots, n$, we have $U(z^*)^{-1} \cdot x^* = 0$ and z^* is a simple zero of $\det U(z)^{-1}$.*

Proof. If the matrix $Q(z) = (\mathcal{Q}_{x_i,a^{(j)}}(z))_{i,j}$ is invertible, then so is $U(z) \in \mathbb{C}(z)^{n \times n}$. Indeed, Theorem 4.1 implies

$$\det(U(z)) = \det(Q(z)) \cdot \left(\mathcal{R}(z)^n \cdot \prod_{j=1}^n \mathcal{S}_{a^{(j)}}(z) \right)^{-1}.$$

For any j , we have

$$U(z) \cdot \begin{pmatrix} 0 \\ \vdots \\ \mathcal{R}(z) \cdot \mathcal{S}_{a^{(j)}}(z) \\ \vdots \\ 0 \end{pmatrix} = \begin{pmatrix} \mathcal{Q}_{x_1, a^{(j)}}(z) \\ \vdots \\ \mathcal{Q}_{x_j, a^{(j)}}(z) \\ \vdots \\ \mathcal{Q}_{x_n, a^{(j)}}(z) \end{pmatrix}$$

by Theorem 4.1. This is an equality of vectors of rational functions. We denote the right-hand side by $Q_j(z)$. Left multiplying by $U(z)^{-1}$ and plugging in $z = z^*$ shows that $(z^*, Q_j(z^*))$ is an eigenpair of $U(z)^{-1}$. Here we use that x^* is a simple toric eigenvector, so that $Q_j(z^*) \neq 0$. It remains to show that, as points in projective space \mathbb{P}^{n-1} , we have $Q_j(z^*) = x^*$. For this, one adapts the proof of [10, Lemma 3.9]. The important step requires [9, Proposition 1.37]. For brevity, we omit technicalities and leave the details to the reader.

To see that z^* is a simple zero of $\det U(z)^{-1}$, we start from the identity

$$(5.3) \quad \det U(z)^{-1} \cdot \det Q(z) = \mathcal{R}^n(z) \cdot \prod_{j=1}^n \mathcal{S}_{a^{(j)}}(z).$$

We have established that $\det U(z)^{-1} = c_1(z - z^*)^\kappa + O((z - z^*)^{\kappa+1})$ near $z = z^*$ for some $c_1 \in \mathbb{C} \setminus \{0\}$ and $\kappa > 0$. Moreover, since $\mathcal{S}_{a^{(j)}}(z^*) \neq 0$ and z^* is a simple zero of $\mathcal{R}(z)$, the right-hand side equals $c_3(z - z^*)^n + O((z - z^*)^{n+1})$ for some $c_3 \in \mathbb{C} \setminus \{0\}$. Since $Q_j(z^*) = x^* \in \mathbb{P}^n$ for all $j = 1, \dots, n$, we know that $\text{rank}(Q(z^*)) = 1$. Therefore, $(z - z^*)$ divides all but one of the invariant factors of $Q(z)$, viewed as a matrix over $\mathbb{C}[z]$. It follows that $\det Q(z) = c_2(z - z^*)^\lambda + O((z - z^*)^{\lambda+1})$ for $\lambda \geq n - 1$. Since $\kappa + \lambda = n$ by (5.3), we must have $\kappa = 1, \lambda = n - 1$, which concludes the proof. \square

Theorem 5.1 shows that the matrix $U(z)$ reduces our problem to a rational eigenvalue problem of the form $U(z)^{-1} \cdot x = 0$, which can be solved using contour integration techniques from section 2. We proceed by discussing how to do this in practice.

The k th moment matrix A_k is given by

$$A_k = \frac{1}{2\pi\sqrt{-1}} \oint_{\partial\Omega} z^k U(z) dz, \quad k = 0, 1, 2, \dots$$

To find the poles of $U(z)$, these matrices are arranged into two block Hankel matrices B_0, B_1 , on which we perform a sequence of standard numerical linear algebra operations. This was explained in section 2. The rank of B_0 equals the number of eigenvalues inside $\partial\Omega$. We emphasize that when $T(x, z) = T(z)$ represents a PEP, the matrix $U(z)$ is given by $T(z)^{-1} \cdot (a^{(1)} \ \dots \ a^{(\ell)})^\top$ and our moment matrices A_k coincide with those used in Beyn's algorithm. In practice, we approximate the moment matrices A_k using numerical integration techniques. We assume that $\partial\Omega$ is parameterized by a differentiable map $\varphi: [0, 2\pi) \rightarrow \mathbb{C}$, so that the k th moment matrix can be written as

$$A_k = \frac{1}{2\pi\sqrt{-1}} \int_0^{2\pi} U(\varphi(t)) \varphi'(t) \varphi^k(t) dt.$$

A standard approach to evaluate this integral numerically is to use the *trapezoidal rule* with $N + 1$ equidistant nodes $t_\ell = \frac{2\pi\ell}{N}$, $\ell = 0, \dots, N$. This gives the approximation $A_{k,N} \approx A_k$:

$$(5.4) \quad A_{k,N} = \frac{1}{\sqrt{-1}N} \sum_{\ell=0}^{N-1} U(\varphi(t_\ell)) \varphi'(t_\ell) \varphi^k(t_\ell).$$

Hence, we need to evaluate $U(z)$ for $z = \varphi(t_\ell), \ell = 0, \dots, N - 1$. We do this efficiently, without explicitly constructing $U(z)$, using *homotopy continuation methods*. Here, we briefly review the basics. For a complete introduction, the reader is referred to the textbook [17].

For fixed $t \in [0, 2\pi)$, the trace vectors $\text{Tr}_{\mathcal{A}_0}(I_{a^{(j)}})|_{z=\varphi(t)}$ are obtained by summing over the solutions to the system of polynomial equations given by $F(x, t) = 0$, where

$$F(x, t) = T(x, \varphi(t)) \cdot x - a^{(j)}(x) = \begin{pmatrix} f_1(x, \varphi(t)) - a_1^{(j)}(x) \\ \dots \\ f_n(x, \varphi(t)) - a_n^{(j)}(x) \end{pmatrix}.$$

By Assumption 3, there are δ solutions. We think of these solutions as paths $x^{(m)} : [0, 2\pi) \rightarrow \mathbb{C}^n$ satisfying $F(x^{(m)}(t), t) = 0, m = 1, \dots, \delta$. These paths are described by a system of ordinary differential equations called the *Dauidenko equation*:

$$(5.5) \quad \frac{dF(x(t), t)}{dt} = J_F(x(t), t) \cdot \frac{dx}{dt} + \frac{\partial F(x(t), t)}{\partial t} = 0,$$

where J_F is the Jacobian matrix whose (j, k) entry is $\frac{\partial f_j}{\partial x_k}$. Each of the paths is uniquely determined by an initial condition specifying $x^{(m)}(t_0) = x^{(m)}(0)$. For computing the trace, we need to evaluate the paths at the discrete points $t_\ell = \frac{2\pi\ell}{N}$. The situation is illustrated by means of a cartoon in Figure 5.1, where $\partial\Omega$ is the unit circle in the complex plane, parameterized by $\varphi(t) = \cos(t) + \sqrt{-1} \cdot \sin(t)$. This is drawn in orange. At each of the points $\varphi(t_\ell)$, represented as black dots on $\partial\Omega$, there are $\delta = 3$ solutions $x^{(m)}(t_\ell), m = 1, \dots, 3$ to $F(x, t_\ell) = 0$. This is illustrated with a dashed line for one choice of ℓ .

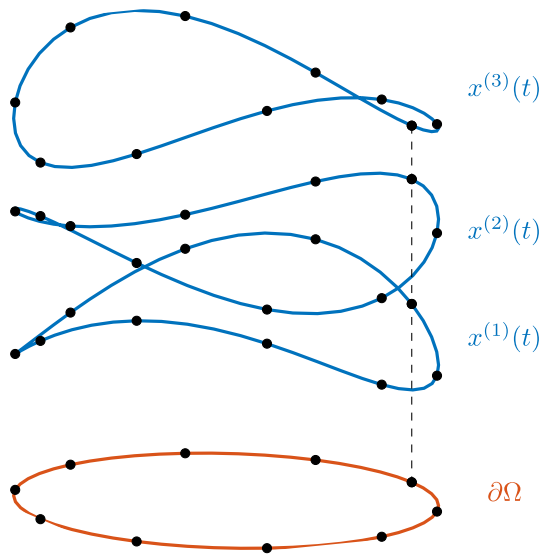


FIG. 5.1. An illustration of the paths $x^{(m)}(t), m = 1, \dots, \delta$ and the discretized paths $x^{(m)}(t_\ell), \ell = 0, \dots, N$ for $\delta = 3$ and $N = 9$. (Figure in color online.)

Downloaded 11/29/23 to 192.16.191.136 . Redistribution subject to SIAM license or copyright; see https://pubs.siam.org/terms-privacy

Approximating $x^{(m)}(t_\ell)$ can be done using numerical techniques for solving the Davidenko equation (5.5). An example is the Euler method, which approximates $x^{(m)}(t_\ell)$ from $x^{(m)}(t_{\ell-1})$ using finite differences. An important remark is that, in our scenario, we have an implicit equation $F(x(t), t) = 0$ satisfied by the solution paths. This allows us, in every step, to refine an approximation $\widetilde{x^{(m)}(t_\ell)}$ for $x^{(m)}(t_\ell)$ using *Newton iteration* on $F(x, t_\ell) = 0$. With a slight abuse of notation, we also write $x^{(m)}(t_\ell)$ for the numerical approximation of $x^{(m)}(t_\ell)$ obtained *after* this refinement. The path values $x^{(m)}(t_\ell)$ are used to evaluate the i th column $\text{Tr}_{\mathcal{A}_0}(I_{a^{(j)}})$ of $U(\varphi(t_\ell))$, by plugging $a = a^{(j)}$ and $\xi = x^{(m)}(t_\ell)$ into (5.1).

We summarize this discussion in Algorithm 5.1 and provide some clarifying remarks. We start by pointing out that Assumption 3 guarantees that for all but finitely many values $z \in \mathbb{C}$, the system of equations $T(x, z) \cdot x - a^{(j)}(x) = 0$ has δ isolated solutions $x \in \mathbb{C}^n$, each with multiplicity one. We assume that the contour $\partial\Omega$ misses these finitely many z -values, which makes sure that the solution paths $x^{(m)}(t)$ do not *cross*, i.e., $x^{(m)}(t) \neq x^{(m')}(t)$ for $m \neq m'$. This can be realized, if necessary, by slightly enlarging Ω . In line 1 of Algorithm 5.1, the starting points $x^{(m)}(t_0)$ are computed. This can be done using any numerical method for solving polynomial systems. Recent eigenvalue methods are described in [2]. In case of many variables, it is favorable to use the *polyhedral homotopies* introduced in [14]. We note that in this step it is crucial that *all* δ solutions are found. An “incomplete” trace which sums over a subset of all solutions will not satisfy the formula of Theorem 4.1. Line 6 is often called the *predictor* step. Our presentation assumes a first order predictor, which uses only $x^{(m)}(t_{\ell-1})$ to compute an approximation for $x^{(m)}(t_\ell)$. In practice, one sometimes uses the path values at $t_{\ell-2}, t_{\ell-3}, \dots$ for more accurate results. It is important to remark that when N is too small, the step size $2\pi/N$ may be too large to track the paths reliably. A bad approximation in line 6 may cause the Newton iteration in line 7 to converge to a *different* path. This phenomenon is called *path jumping*. To remedy this, one could take some “extra” steps between $t_{\ell-1}$ and t_ℓ . Recent studies in the direction of *adaptive stepsize* algorithms are [20, 21]. Details are beyond the scope of this paper. In our implementation, the algorithm in [21] decides how many steps to take between $t_{\ell-1}$ and t_ℓ . Line 7 is called the *corrector* step, and Algorithm 5.1 is a blueprint for a *predictor-corrector* scheme; see, e.g., [20, Alg. 2.1].

Algorithm 5.1 Evaluating the j th column of $U(z)$ at $z = \varphi(t_\ell), \ell = 0, \dots, N - 1$.

```

1: Compute  $\delta$  start solutions  $x^{(m)}(t_0), m = 1, \dots, \delta$  satisfying  $F(x^{(m)}(t_0), t_0) = 0$ 
2:  $\text{Tr}_{\mathcal{A}_0}(I_{a^{(j)}})|_{z=\varphi(t_0)} = \left( \sum_{m=1}^{\delta} (x^{(m)}(t_0))_i \right)_{i=1, \dots, n}$ 
3:  $\ell \leftarrow 0$ 
4: while  $\ell \leq N$  do
5:   for  $m = 1, \dots, \delta$  do
6:      $\widetilde{x^{(m)}(t_\ell)} \leftarrow$  an approximation for  $x^{(m)}(t_\ell)$  obtained from  $x^{(m)}(t_{\ell-1})$ 
7:      $x^{(m)}(t_\ell) \leftarrow$  refine  $\widetilde{x^{(m)}(t_\ell)}$  using Newton iteration
8:   end for
9:    $\text{Tr}_{\mathcal{A}_0}(I_{a^{(j)}})|_{z=\varphi(t_\ell)} = \left( \sum_{m=1}^{\delta} (x^{(m)}(t_\ell))_i \right)_{i=1, \dots, n}$ 
10:   $\ell \leftarrow \ell + 1$ 
11: end while

```

Algorithm 5.2 Contour integration for the PEPv.

- 1: Choose $M \in \mathbb{N}$ such that $M \cdot n$ is larger than the expected number of eigenvalues in Ω .
 - 2: Use Algorithm 5.1 to compute $U(z)$ columnwise for each $z = \varphi(t_\ell)$
 - 3: $A_{k,N} \leftarrow \frac{1}{\sqrt{-1}^N} \sum_{\ell=0}^{N-1} U(\varphi(t_\ell)) \varphi'(t_\ell) \varphi^k(t_\ell)$ for $k = 0, \dots, 2M - 1$
 - 4: Construct block Hankel matrices $B_{0,N}$ and $B_{1,N}$ as in (2.2)
 - 5: Compute the SVD $B_{0,N} = V \Sigma W^H$ with $\Sigma = \text{diag}(\sigma_1, \sigma_2, \dots, \sigma_{Mn})$
 - 6: Estimate $\text{rank}(B_{0,N})$: find $0 < l \leq Mn$ s.t. $\sigma_1 \geq \sigma_2 \geq \dots \geq \sigma_l > \sigma_{l+1} \approx \dots \approx \sigma_{Mn} \approx 0$.
 - 7: **if** $l = Mn$ **then**
 - 8: Increase M and go back to step 1.
 - 9: **else**
 - 10: $V_0 \leftarrow V(1 : Mn, 1 : l)$, $W_0 \leftarrow W(1 : Mn, 1 : l)$, $\Sigma_0 \leftarrow \text{diag}(\sigma_1, \dots, \sigma_l)$
 - 11: $D \leftarrow V_0^H B_{1,N} W_0 \Sigma_0^{-1}$
 - 12: Compute all eigenvalues of D
 - 13: Accept an eigenpair (y_j^*, z_j^*) of D as a solution (x_j^*, z_j^*) of the PEPv with corresponding eigenvector $x_j^* = V_0^{[1]} y_j^*$ if $T(x_j^*, z_j^*) \cdot x_j^*$ is smaller than a given tolerance.
 - 14: **end if**
-

The complete algorithm to identify solutions of the PEPv using contour integration is summarized in Algorithm 5.2. Note that the only difference from Beyn’s algorithm as described in [3] is the calculation of $A_{k,N}$ in lines 2 and 3.

6. Complexity. In this section, we discuss the complexity of the contour integration algorithm presented in section 5. We split the algorithm into two major steps:

1. Evaluate the moment matrices A_0, \dots, A_{2M-1} .
2. Extract the eigenvalues from these moment matrices.

In step 2, one constructs the matrices B_0, B_1 from (2.2). These are of size $M \cdot n$, and M is chosen such that $M \cdot n \geq \delta(\Omega)$, where $\delta(\Omega)$ is the number of eigenvalues inside Ω . The eigenvalues are then extracted from B_0, B_1 by computing an SVD; see section 2. The cost is $O(M^3 \cdot n^3)$. The most favorable situation for our method is when $\delta(\Omega) \approx M \cdot n \ll \hat{\delta}$.

Step 1 uses numerical homotopy continuation. Continuing to work under Assumption 3, it requires tracking $n \cdot \delta = n \cdot \text{MV}(P_1, \dots, P_n)$ solution paths. The homotopy is used to evaluate $U(\varphi(t_\ell))$ as discussed in section 5. The moment matrices A_k are then approximated via (5.4). In our analysis, we assume that the number of nodes N is fixed. Moreover, we ignore the complexity of computing $A_{k,N}$ from $U(\varphi(t_\ell))$, as it is negligible compared to the cost of tracking our $n \cdot \delta$ paths.

As an alternative to our method, one could also use homotopy continuation to solve the system of equations $T(x, z) \cdot x = 0$ directly. Here one dehomogenizes, e.g., by setting $x_1 = 1$, to obtain a system of n equations in n variables. The number of paths tracked by homotopy continuation is at least the total number of eigenvalues, which is denoted $\hat{\delta}$ in what follows. The eigenpairs whose eigenvalues lie outside Ω can then be discarded. Below, we will refer to this approach as the *naive* approach. The reader is referred to the standard textbook [17] for more details on homotopy continuation for solving polynomial systems.

To compare our method to this naive approach, the number $n \cdot \delta$ should be compared to the total number $\hat{\delta}$ of eigenvalues of $T(x, z)$. However, we warn the reader that one cannot straightforwardly draw conclusions about the computation time by simply comparing $n \cdot \delta$ with $\hat{\delta}$. For instance, it might be favorable to solve n problems with $\delta < \hat{\delta}$ solutions rather than one problem with $\hat{\delta}$ solutions, even if $n \cdot \delta > \hat{\delta}$. Below, we compute the number of paths $n \cdot \delta$ for two families of PEPv's. The first one is inspired by Theorems A.1 and A.2, where $d_1 = \dots = d_n$. The second one is a family of systems of rational function equations from [5], which can be solved using a slight modification of our method.

6.1. Unmixed, dense equations. We consider the case where $T(x, z) \cdot x = (f_1(x, z), \dots, f_n(x, z))^T$ comes from the polynomial system $f_1 = \dots = f_n = 0$, where each f_i is homogeneous of degree $d + 1$ in x , and of degree e in z . We assume that $x_j^{d+1}, j = 1, \dots, n$, appear in each of the f_i . First, we also choose the polynomials $a_i(x) \in \mathbb{C}[x]_d$ such that $x_j^d, j = 1, \dots, n$, appear in each of them. This is the situation of Theorem A.1, which states that the polynomial $\mathcal{S}_a(z)$ from Theorem 4.1 for such a PEPv is constant. We compute the numbers $n \cdot \delta$ and $\hat{\delta}$ for this setup.

PROPOSITION 6.1. *Let $f_1, \dots, f_n, a_1, \dots, a_n$ be as in Theorem A.1. We have*

$$n \cdot \delta = n \cdot ((d + 1)^n - d^n), \quad \hat{\delta} = e \cdot n \cdot (d + 1)^{n-1}.$$

Proof. By the multihomogeneous version of Bézout's theorem [17, Theorem 8.4.7], the total number of eigenvalues, i.e., solutions to $f_1 = \dots = f_n = 0$ is $\hat{\delta} = e \cdot n \cdot (d + 1)^{n-1}$. To compute δ , consider the polytope $P = P_1 = \dots = P_n \subset \mathbb{R}^n$, given by (A.1), with $d_i = d$. By Kushnirenko's theorem [6, Chapter 7, sect. 5, Exercise 5], the number δ is the lattice volume of P . This is given by $\delta = (d + 1)^n - d^n$. \square

It follows that, for large d , the ratio $(n \cdot \delta)/\hat{\delta}$ tends to n/e . Hence, our method tracks significantly fewer solution paths when $e \gg n$. We note that, for small d , this conclusion is pessimistic. For instance, if $d = 2$, we find that $(n \cdot \delta)/\hat{\delta} \approx 2/e$.

A smaller number of paths $n \cdot \delta$ is obtained when the $a_i(x)$ are chosen as in Theorem A.2: $a_i = c_i x^\beta$ consists of one term of degree d , with $c_i \neq 0$. The computation is similar to the proof of Proposition 6.1, noting that the lattice volume of a pyramid of lattice height 1 equals the $(n - 1)$ -dimensional lattice volume of its base.

PROPOSITION 6.2. *Let $f_1, \dots, f_n, a_1, \dots, a_n$ be as in Theorem A.2. We have*

$$n \cdot \delta = n \cdot (d + 1)^{n-1}.$$

Propositions 6.1 and 6.2 lead us to conclude that the methods presented in this paper are effective only when the degree in the eigenvalue variable is large. This situation arises, for instance, when the PEPv comes from a polynomial approximation of a set of equations that depends transcendently on z . We will show an example in section 7.3. Proposition 6.2 also shows that the complexity of our method increases sensitively with n and d . Still, as our experiments in section 7 show, it can be used to solve challenging instances.

6.2. Rational functions. We now discuss an example where the entries of the matrix $T(x, z)$ are homogeneous *rational* functions in x . More precisely, consider a rational map $T: \mathbb{P}^{n-1} \times \mathbb{C} \dashrightarrow \mathbb{C}^{n \times n}$ of the form

$$(6.1) \quad T(x, z) = T_0(z) + \frac{r_1(x)}{s_1(x)} T_1 + \dots + \frac{r_m(x)}{s_m(x)} T_m,$$

where $T_0(z) = A + z \cdot B$ with $A, B \in \mathbb{C}^{n \times n}$, and $r_i(x), s_i(x)$ are linear forms in x . The associated *rational eigenvalue problem with eigenvector nonlinearities* (REPV) is

$$(6.2) \quad \text{find } (x^*, z^*) \in (\mathbb{P}^{n-1} \setminus V_{\mathbb{P}^{n-1}}(s_1 \cdots s_m)) \times \mathbb{C} \text{ such that } T(x^*, z^*) \cdot x^* = 0.$$

Here we use the standard notation $V_X(f) = \{x \in X \mid f(x) = 0\}$. The problem (6.2) was studied in [5]. We discuss here how our methods can be used to solve this REPV. We point out that, in this case, the problem cannot be turned into a PEPV by clearing denominators, as this typically introduces infinitely many spurious eigenvectors.

Recall that the degree of a rational function r/s is the difference of the $\deg(r)$ and $\deg(s)$. The rows of T are homogeneous of degree $d = 0$ in x . Consistently with our approach for PEPV's, we consider the equation $T(x, z) \cdot x - a = (f_1 - a_1, \dots, f_n - a_n)^\top = 0$, where $a = (a_1, \dots, a_n)^\top \in \mathbb{C}^n$ is a generic vector of complex constants. The matrix $U(z)$ from (5.2) is constructed by summing over the δ solutions. Essentially, the reason why this works is that these rational function equations are equivalent to a system of polynomial equations in $m + n$ variables. This is used in the proof of the following theorem, which predicts δ .

THEOREM 6.3. *For T as in (6.1) and generic $z^* \in \mathbb{C}, a \in \mathbb{C}^n$, the system of equations $T(x, z^*) \cdot x - a = 0$ has at most δ isolated solutions in $(\mathbb{C}^n \setminus V_{\mathbb{C}^n}(s_1 \cdots s_m))$, with*

$$\delta = \sum_{k=0}^{\min(n-1, m)} \binom{n-1}{k} \cdot \binom{m}{k}.$$

Sketch of proof. The system of rational function equations $T(x, z) \cdot x - a = 0$ is equivalent to the system of $n + m$ polynomial equations

$$(6.3) \quad (T_0 + \lambda_1 T_1 + \cdots + \lambda_n T_n) \cdot x - a = 0, \quad s_i(x) \lambda_i - r_i(x) = 0, \quad i = 1, \dots, m,$$

where $\lambda_1, \dots, \lambda_m$ are new variables and $T_0 = T_0(z)$. The entries of $(T_0 + \lambda_1 T_1 + \cdots + \lambda_n T_n) \cdot x - a$ all have the same Newton polytope, denoted $P \subset \mathbb{R}^{m+n}$. The equation $s_i(x) \lambda_i - r_i(x)$ has Newton polytope $\Delta_n \times L_i$, where $\Delta_n = \text{Conv}(e_1, \dots, e_n) \subset \mathbb{R}^n$ and $L_i = \text{Conv}(0, e_i) \subset \mathbb{R}^m$. By the BKK theorem [6, Chapter 7, sect. 5], the number of isolated solutions to (6.3) is bounded by the mixed volume $\delta = \text{MV}(P, \dots, P, \Delta_n \times L_1, \dots, \Delta_n \times L_m)$. Here P is listed n times. Multilinearity and symmetry of the mixed volume gives the equality

$$\delta = \sum_{k=0}^m \binom{m}{k} \text{MV}(P, \dots, P, \Delta_n, \dots, \Delta_n, L_{k+1}, \dots, L_m).$$

Since Δ_n has dimension $n - 1$, all terms with $k > n - 1$ are zero. It remains to show that for $k \leq \min(n - 1, m)$, we have

$$\text{MV}(P, \dots, P, \Delta_n, \dots, \Delta_n, L_{k+1}, \dots, L_m) = \binom{n-1}{k}.$$

This number counts solutions to $(T_0 + \lambda_1 T_1 + \cdots + \lambda_n T_n) \cdot x - a = 0$ after plugging in random values for $\lambda_{k+1}, \dots, \lambda_m$ and replacing x_{n-k+1}, \dots, x_n by generic linear forms in x_1, \dots, x_{n-k} . What is left is a system of n equations in the variables $(x_1, \dots, x_{n-k}, \lambda_1, \dots, \lambda_k)$. It has at most $\binom{n-1}{k}$ solutions by the multihomogeneous version of Bézout's theorem. \square

By [5, Theorem 3.1], the total number of eigenvalues of (6.1) is $\hat{\delta} = \binom{n+m}{m+1}$. Although $\delta < \hat{\delta}$, we have $n \cdot \delta > \hat{\delta}$. We will illustrate this with an example in section 7. We leave the question whether and when our method is advantageous for solving this type of REPV as a topic for future research.

7. Numerical experiments. In this section we present several numerical examples illustrating the results presented above. Our algorithm has two important parameters that impact the numerical performance: the number $N + 1$ of discretization points on the contour to evaluate the integral, and the number of moment matrices $2M$. In the experiments below, we will investigate the influence of these parameters on the accuracy. We assess the quality of an approximate eigenpair (x^*, z^*) by its residual $r^* = \|T(x^*, z^*) \cdot x^*\| / \|x^*\|$. The presented results are generated by an implementation in Julia (v1.6) using `HomotopyContinuation.jl` (v2.6.4) [4]. The source code is available online to reproduce all results.¹

7.1. Experiment 1. Consider the PEPv $T(x, z) \cdot x = 0$ where $T(x, z)$ has size 3×3 and each row is of degree $d = 2$ in x and $e = 4$ in z . The coefficients are randomly generated in order to obtain a generic system. The contour enclosing the target domain Ω is shown in Figure 7.1 together with the exact eigenvalues in the neighborhood of Ω .

The impact of the number of discretization points $N + 1$ is the most intuitive: the more points, the higher the accuracy of the detected eigenvalues in Ω . There is a less intuitive impact that has been observed in contour integration for nonlinear eigenvalue problems [22]. When the contour integral is approximated with a low number of points, it is possible that eigenvalues outside the contour are detected. Evaluating the contour integral with 1000 points detects only the four eigenvalues in Ω with average residual in the order of magnitude of machine precision. However, evaluating the contour integral with 100 points detects 14 eigenvalues depicted in Figure 7.1: four eigenvalues in Ω with average residual of $\approx 10^{-11}$ and eight eigenvalues outside the target domain with residual varying from 10^{-9} to 10^{-5} depending on the distance from

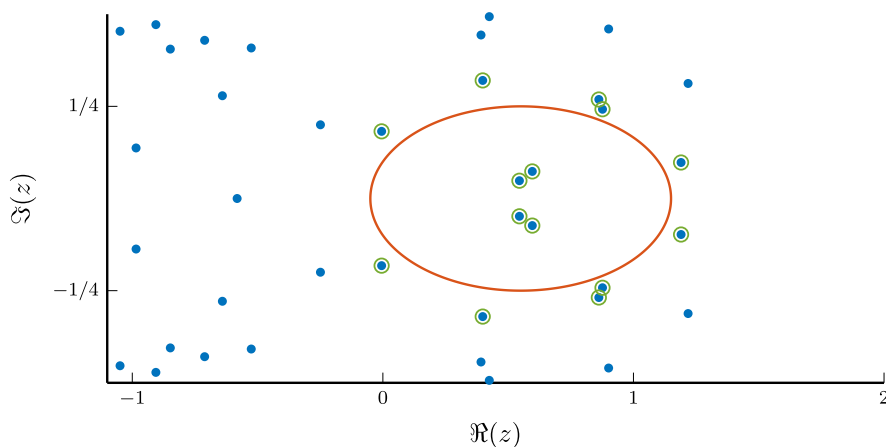


FIG. 7.1. Eigenvalues (\bullet) inside the target domain defined by the contour (---) and the extracted values by contour integration (\circ) for experiment 1. (Figure in color online.)

¹github.com/robclaes/contour-integration.

the contour. This phenomenon is best explained via the relation between numerical integration and filter functions on \mathbb{C} ; see [22] for details.

An obvious impact of the number of moment matrices can be seen in (2.2): the maximum number of eigenvalues that can be detected is Mn . Therefore, M should be large enough to detect at least the expected number of eigenvalues in Ω . However when a low number of discretization points is chosen, extra care must be taken when choosing the number of moment matrices: the algorithm will detect additional eigenvalues outside Ω which may lead to more eigenvalues than the number of eigenvalues that can be detected for a given M . For the specific instance here, we selected $M = 9$ which leads to a maximum of $Mn = 27$ detectable eigenvalues. In the case with 100 discretization points this upper bound is large enough to detect the 14 eigenvalues. When we set $M = 2$ – which should suffice for the expected four eigenvalues in Ω – with 100 discretization points, the eigenvalues outside Ω perturb the result leading to an average residual of the four eigenvalues in Ω of 10^{-3} .

Since the degree of the polynomials is the same for each row, we select the polynomials a_i in accordance with Theorem A.2, i.e., a_i is a monomial in x of degree $d = 2$. By Proposition 6.2, this leads to $n \cdot \delta = n \cdot (d + 1)^{n-1} = 27$ tracked paths, which is smaller than the expected number of tracked paths when using random polynomials: $n \cdot \delta = n \cdot ((d + 1)^n - d^n) = 57$.

7.2. Experiment 2. Consider the PEPv $T(x, z) \cdot x = 0$ where $T(x, z)$ has size 10×10 and each row is of degree $d = 1$ in x and $e = 5$ in z . The coefficients are randomly generated. The contour enclosing the target domain Ω is shown in Figure 7.2a together with the exact eigenvalues in the neighborhood of Ω . This is a very nontrivial problem since the total number of solutions of the PEPv equals $\hat{\delta} = 25600$ and they are almost all clustered around the origin of the complex plane. The selected contour is a circle with center at the origin and a radius of 0.1 which encircles 44 eigenvalues of the problem.

Since the neighborhood of the target region Ω is densely scattered with eigenvalues, we select a relatively high number of integration points $N + 1 = 400$ to increase

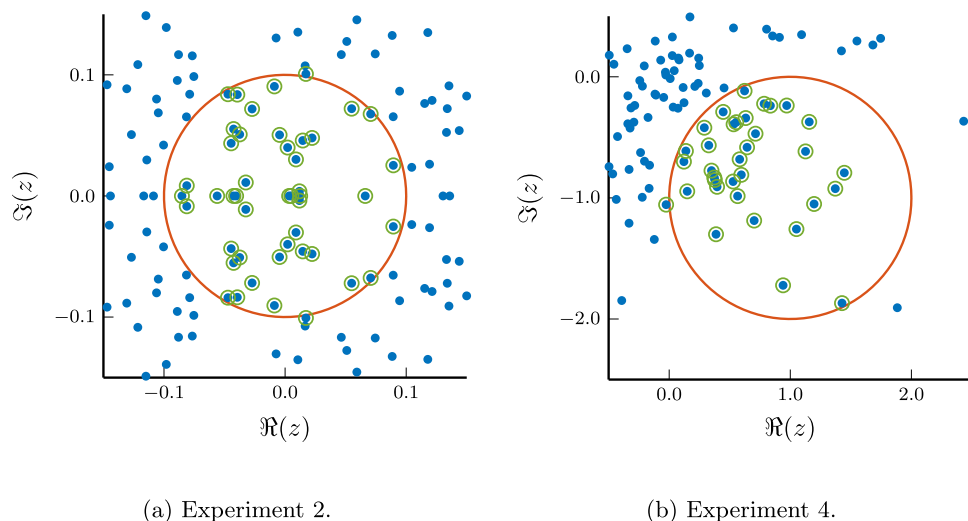


FIG. 7.2. Eigenvalues (\bullet) inside the target domain defined by the contour (---) and the extracted values by contour integration (\circ). (Figure in color online.)

the sharpness of the integration filter as discussed in the previous example. Given the high number of integration points, a maximum of $2M = 10$ moment matrices should suffice to capture the 44 expected eigenvalues in Ω . The result is shown in Figure 7.2a: a total of 46 detected eigenvalues: 44 inside Ω and 2 just outside the target region. The residual for the extracted eigenpairs varies from 10^{-4} to 10^{-8} . In accordance with Theorem A.2, we selected a_i as a monomial of degree $d = 1$ which leads to $n \cdot \delta = n \cdot (d + 1)^{n-1} = 5120$ tracked paths for our method (Proposition 6.2). Finding all 25600 solutions with standard homotopy continuation takes roughly 2390 seconds to compute, while our approach with 400 interpolation points takes 1120 seconds. (Both timings result from a single-thread implementation in Julia.)

7.3. Experiment 3. Consider the system of equations $T(x, z) \cdot x = 0$ given by

$$(7.1) \quad T(x, z) = \begin{pmatrix} x_1^2 x_2 & -2\sqrt{-1}x_1^2 x_2 \cos(z) \\ -x_2^2 \cos(z^2) & 2x_2^2 \sin(3z) \end{pmatrix}.$$

Note that this system is not polynomial in z , but, in practice, the system is solved by an implicit substitution of Maclaurin series of high order for the sine and cosine functions. This approach leads to a PEPv that is of high degree in z . We expect an infinite number of solutions since the trigonometric functions can be expressed by their Maclaurin series in z . We use 100 discretization points for the contour, and $2M = 16$ moment matrices. The a_i are selected as random monomials in x that have the same degree as the polynomials in the corresponding row of $T(x, z)$, similarly as in Theorem A.2. This leads to four tracked paths, instead of 10 for random polynomials. Figure 7.3 shows the impact of the number of discretization points on the residual of the 11 extracted solutions. As stated in experiment 1, increasing the number of discretization points leads to a decrease in the residual.

7.4. Experiment 4. Consider the REpv (6.1) of dimension $n = 10$ with $m = 2$ rational terms where all coefficients are randomly generated. A problem with these dimensions is expected to have $\hat{\delta} = \binom{n+m}{m+1} = 220$ eigenvalues. According to Theorem 6.3 we need to track $n \cdot \delta = 550$ paths. As depicted in Figure 7.2e, all 33 eigenvalues in the contour are detected with a residual ranging from 10^{-8} to 10^{-12} , and one eigen-

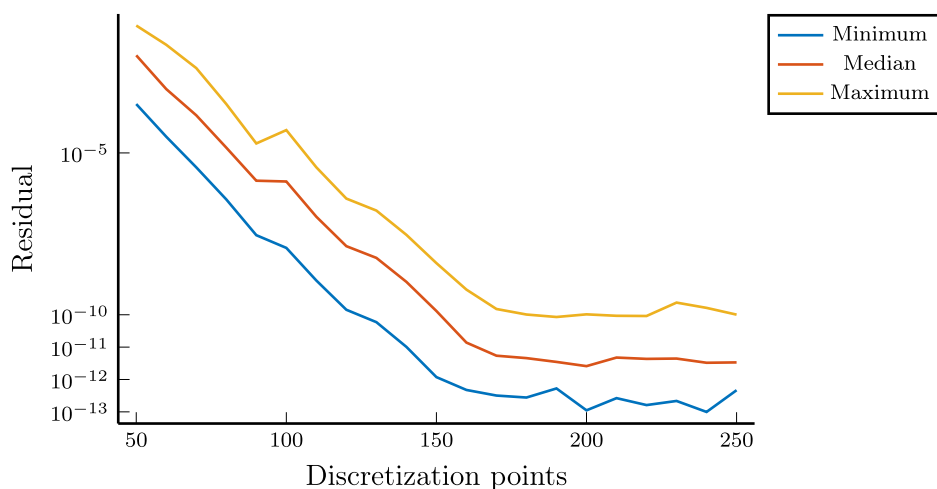


FIG. 7.3. Impact of number of discretization points on residuals for experiment 3.

value outside of the contour with a residual of 10^{-6} . This result is obtained using $N + 1 = 400$ nodes, and $2M = 10$ moment matrices.

7.5. Experiment 5. Our final example shows explicitly how to convert a system of polynomial equations into a PEPv. We illustrate this by means of an example from computational biology. In a formulation taken from [12, sect. 3], the equilibrium conformations of a cyclic six-atom molecule are encoded by the solutions of the polynomial system $\hat{f}_1 = \hat{f}_2 = \hat{f}_3 = 0$, where

$$\begin{aligned} \hat{f}_1 &= \beta_{11} + \beta_{12}t_2^2 + \beta_{13}t_3^2 + \beta_{14}t_2t_3 + \beta_{15}t_2^2t_3^2, \\ \hat{f}_2 &= \beta_{21} + \beta_{22}t_3^2 + \beta_{23}t_1^2 + \beta_{24}t_1t_3 + \beta_{25}t_1^2t_3^2, \\ \hat{f}_3 &= \beta_{31} + \beta_{32}t_1^2 + \beta_{33}t_2^2 + \beta_{34}t_1t_2 + \beta_{35}t_1^2t_2^2. \end{aligned}$$

Only *real* solutions $(t_1, t_2, t_3) \in \mathbb{R}^3$ are relevant for the application. The parameters β_{ij} are the entries of a 3×5 -matrix β , which depends on the molecule under consideration. The coefficients used for *cyclohexane* in [12] are

$$\beta = \begin{pmatrix} -310 & 959 & 774 & 1389 & 1313 \\ -365 & 755 & 917 & 1451 & 1269 \\ -413 & 837 & 838 & 1655 & 1352 \end{pmatrix}.$$

Our system has three equations in three unknowns. The first step to formulate this as a PEPv is to let one of the variables play the role of *eigenvalue*. For no specific reason, we choose $z = t_2$. We view $\hat{f}_i(t_1, t_3)$ as polynomials in t_1, t_3 , with coefficients in $K = \mathbb{C}(z)$. Note that \hat{f}_1 and \hat{f}_3 have degree two, while \hat{f}_2 has degree four. Next, we homogenize the equations

$$f_1 = x_3^2 \cdot \hat{f}_1 \left(\frac{x_1}{x_3}, \frac{x_2}{x_3} \right), \quad f_2 = x_3^4 \cdot \hat{f}_2 \left(\frac{x_1}{x_3}, \frac{x_2}{x_3} \right), \quad f_3 = x_3^2 \cdot \hat{f}_3 \left(\frac{x_1}{x_3}, \frac{x_2}{x_3} \right).$$

The equations $f_1 = f_2 = f_3 = 0$ are equivalent to $T(x, z) \cdot x = 0$, with

$$(7.2) \quad T(x, z) = \begin{pmatrix} 0 & (\beta_{13} + \beta_{15}z^2)x_2 + \beta_{14}zx_3 & (\beta_{11} + \beta_{12}z^2)x_3 \\ (\beta_{23}x_1 + \beta_{24}x_2)x_3^2 & (\beta_{25}x_1^2 + \beta_{22}x_3^2)x_2 & \beta_{21}x_3^3 \\ (\beta_{32} + \beta_{35}z^2)x_1 + \beta_{34}zx_3 & 0 & (\beta_{31} + \beta_{33}z^2)x_3 \end{pmatrix}.$$

An eigenpair (x^*, z^*) with $x_3^* \neq 0$ gives the solution $t_1 = x_1^*/x_3^*, t_2 = z^*, t_3 = x_2^*/x_3^*$ to the original equations $\hat{f}_1 = \hat{f}_2 = \hat{f}_3 = 0$. As reported in [12, sect. 3], there are 16 complex solutions, of which 4 are real. Our method finds (only!) the real solutions by choosing $\Omega = \{z \in \mathbb{C} \mid |z| < 0.4\}$. Our solutions agree with those reported in [12]. The columns of

$$\begin{pmatrix} -0.368436 & 0.712646 & -0.712646 & 0.368436 \\ -0.319725 & -0.0103841 & 0.0103841 & 0.319725 \\ -0.296956 & -0.623453 & 0.623453 & 0.296956 \end{pmatrix}$$

are the approximate solutions (t_1, t_2, t_3) . Note that the t_2 -coordinates lie inside Ω . We point out that these simple equations can be solved rapidly using standard methods, without too much computational overhead coming from the twelve biologically meaningless solutions. We chose this system of equations to demonstrate how to transition between polynomial equations and PEPv's. In larger examples, we do expect our method to outperform standard solvers. This was illustrated in section 7.2.

8. Conclusions. We presented a new contour integration method for solving polynomial eigenvalue problems with eigenvector nonlinearities and developed its first theoretical foundations. The eigenvalues are the roots of a resultant polynomial. We showed that, under suitable assumptions, this polynomial equals the denominator of the trace obtained by summing over the solutions to a modified system of equations. This can be evaluated along a contour using numerical homotopy continuation techniques. This way, we can extract eigenvalues in a compact domain and their corresponding eigenvectors by numerical contour integration. We derived the number of homotopy continuation paths that need to be tracked for two classes of problems. This governs, to a certain extent, the complexity of our method. However, a direct comparison with the total number of eigenvalues is not very meaningful since the difficulty and computational cost of tracking a single path may differ greatly. A comparative study on the total computational cost is an interesting topic for future research, together with a study on the applicability of other NEP methods on the compound trace matrix $U(z)$.

Appendix A. Appendix. This appendix identifies two families of PEPv for which the polynomial $\mathcal{S}_a(z)$ in Theorem 4.1 is constant. For any point ω in \mathbb{Z}^n and any finite subset $\mathcal{C} \subset \mathbb{Z}^n$, let

$$\mathcal{C}^\omega = \left\{ \gamma \in \mathcal{C} \mid \langle \omega, \gamma \rangle = \min_{\gamma' \in \mathcal{C}} \langle \omega, \gamma' \rangle \right\}.$$

Here $\langle \cdot, \cdot \rangle$ is the dot product. For a polynomial $f = \sum_{\gamma \in \mathcal{C}} c_\gamma x^\gamma$ supported in \mathcal{C} , we write f^ω for the *leading form* of f w.r.t. ω :

$$f^\omega = \sum_{\gamma \in \mathcal{C}^\omega} c_\gamma x^\gamma.$$

Let \mathcal{C}_i be the support of $f_i - a_i$, as in section 4, and let $P = P_1 + \dots + P_n$ be the Minkowski sum of the Newton polytopes $P_i = \text{Conv}(\mathcal{C}_i) \subset \mathbb{R}^n$. In the proof of Theorem 4.1 we derived

$$\mathcal{S}_a(z) = C^{-1} \cdot \prod_{\omega \neq \omega^*} R_{\mathcal{C}_1^\omega, \dots, \mathcal{C}_n^\omega}((f_1 - a_1)^\omega, \dots, (f_n - a_n)^\omega)^{\delta_\omega},$$

where ω ranges over the inner facet normals to P . It follows from the definition of δ_ω in [8, sect. 2] that the only facet normals ω for which $\delta_\omega \neq 0$ are those for which $0 \notin \mathcal{C}_0^\omega$. This gives a sufficient condition for $\mathcal{S}_a(z) \in \mathbb{C} \setminus \{0\}$. Let $P_0 = \text{Conv}(\mathcal{C}_0)$ be the standard simplex in \mathbb{R}^n . If the monomials $x_j^{d_i+1}, j = 1, \dots, n$, appear in f_i , and $x_j^{d_i}$ appear in a_i , then

$$(A.1) \quad P_i = \text{Conv}(\mathcal{C}_i) = \text{cl}((d_i + 1) \cdot P_0 \setminus (d_i \cdot P_0)),$$

where $\text{cl}(\cdot)$ denotes the Euclidean closure in \mathbb{R}^n .

THEOREM A.1. *Let $T(x, z) \cdot x = (f_1, \dots, f_n)^\top = 0$ be a PEPv satisfying Assumption 2, with $\deg(f_i) = d_i + 1$. Let $a_i \in \mathbb{C}[x]_{d_i}$ be such that I_a satisfies Assumption 3 and $P_i = \text{Conv}(\mathcal{C}_i) = \text{cl}((d_i + 1) \cdot P_0 \setminus (d_i \cdot P_0))$. Then $\mathcal{S}_a(z)$ in Theorem 4.1 is a nonzero complex constant.*

Proof. The theorem follows from the fact that, under the assumption (A.1), the facet normals of $P = P_1 + \dots + P_n$ are

$$(A.2) \quad \omega^* = (-1, \dots, -1), \quad \omega_0 = (1, \dots, 1), \quad \omega_1 = (1, 0, \dots, 0), \\ \omega_2 = (0, 1, \dots, 0), \quad \omega_n = (0, 0, \dots, 1).$$

Out of these, only for $\omega = \omega^*$ we have $0 \notin \mathcal{C}_0^\omega$. \square

We present one more example of a family of PEPv's for which $S_a(z) \in \mathbb{C} \setminus \{0\}$. We assume that all f_i are of the same degree $d+1$ and such that x_j^{d+1} appears in f_j for all j . We let $a_i = c_i x^\beta$ consist of one term of degree d , with $c_i \neq 0$. The resulting polytopes P_i are all equal to a pyramid of height one over the simplex $(d+1) \cdot \text{Conv}(e_1, \dots, e_n)$.

THEOREM A.2. *Let $T(x, z) \cdot x = (f_1, \dots, f_n)^\top = 0$ be a PEPv satisfying Assumption 2, with $\deg(f_i) = d + 1$. Let $a_i(x) = c_i x^\beta \in \mathbb{C}[x]_d$ be such that I_a satisfies Assumption 3. Then $\mathcal{S}_a(z)$ in Theorem 4.1 is a nonzero complex constant.*

Proof. The polytope $P = P_1 + \dots + P_n = n \cdot P_1$ has $n + 1$ normal vectors. All of these are nonnegative, except $\omega^* = (-1, \dots, -1)$. Therefore, only ω^* satisfies $0 \notin C_0^\omega$. \square

If $\text{Conv}(\mathcal{A}_1) = \dots = \text{Conv}(\mathcal{A}_n)$, the argument in the proof of Theorem A.2 can be used to construct more general situations in which $P_1 = \dots = P_n$ is a pyramid over $\text{Conv}(\mathcal{A}_i)$ and $\mathcal{S}_a(z) \in \mathbb{C} \setminus \{0\}$. We do not work this out explicitly. Here is an example where $\mathcal{S}_a(z) \notin \mathbb{C} \setminus \{0\}$.

Example A.1. The polytope $P = P_1 + P_2 + P_3$ from the PEPv in Example 4.1 is shown in Figure A.1. There are six facets. Their normal vectors ω_i in the dual lattice $(\mathbb{Z}^3)^\vee \simeq \mathbb{Z}^3$ are

$$(A.3) \quad \begin{aligned} \omega_1 = (0, 0, 1), \quad \omega_2 = -(1, 0, 1), \quad \omega_3 = -(1, 1, 1), \quad \omega_4 = (1, 0, 0), \\ \omega_5 = (1, 1, 1), \quad \omega_6 = (0, 1, 0). \end{aligned}$$

Here $\omega^* = \omega_3$. The only other facet normal for which $0 \notin C_0^{\omega_i}$ is ω_2 . We calculate

$$C_1^{\omega_2} = C_2^{\omega_2} = \{(1, 0, 0), (0, 0, 1)\}, \quad C_3^{\omega_2} = \{(1, 0, 0), (0, 0, 1), (0, 1, 1), (1, 1, 0)\}.$$

The corresponding face equations are $f_1^{\omega_2} = f_2^{\omega_2} = f_3^{\omega_2} = 0$, with

$$f_1^{\omega_2} = x_1 + x_3, \quad f_2^{\omega_2} = 2x_1 + zx_3, \quad f_3^{\omega_2} = (z + 1)x_2x_3 + x_1x_2 - b_{31}x_1 - b_{33}x_3.$$

These have a nontrivial solution if and only if the determinant of the linear system $f_1^{\omega_2} = f_2^{\omega_2} = 0$ vanishes. This explains $R_{C_1^{\omega_2}, C_2^{\omega_2}, C_3^{\omega_2}} = z - 2$, which gives the extraneous factor in the denominator of (4.2).

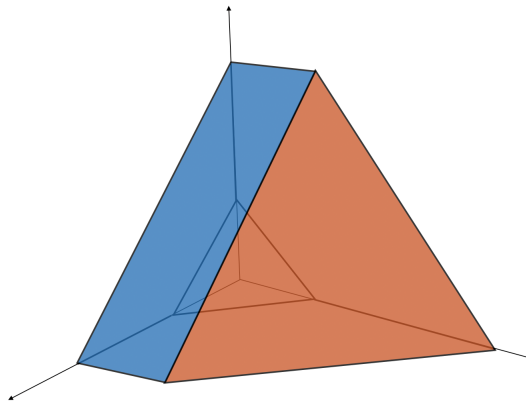


FIG. A.1. The polytope P from Example A.1. The facets corresponding to ω_2 and ω_3 are the quadrilateral and triangle colored in blue and orange, respectively. (Figure in color online.)

Downloaded 11/29/23 to 192.16.191.136 . Redistribution subject to SIAM license or copyright; see https://pubs.siam.org/terms-privacy

Acknowledgments. We thank two anonymous referees for their helpful comments on a previous version of this manuscript. We would also like to thank Paul Breiding for his help with `HomotopyContinuation.jl`, and Carlos D’Andrea for insightful discussions.

REFERENCES

- [1] J. ASAKURA, T. SAKURAI, H. TADANO, T. IKEGAMI, AND K. KIMURA, *A numerical method for nonlinear eigenvalue problems using contour integrals*, JSIAM Lett., 1 (2009), pp. 52–55.
- [2] M. R. BENDER AND S. TELEN, *Yet Another Eigenvalue Algorithm for Solving Polynomial Systems*, preprint, <https://arxiv.org/abs/2105.08472>, 2021.
- [3] W.-J. BEYN, *An integral method for solving nonlinear eigenvalue problems*, Linear Algebra Appl., 436 (2012), pp. 3839–3863.
- [4] P. BREIDING AND S. TIMME, *HomotopyContinuation.jl: A package for homotopy continuation in julia*, in International Congress on Mathematical Software, Springer, Cham, 2018, pp. 458–465.
- [5] R. CLAES, E. JARLEBRING, K. MEERBERGEN, AND P. UPADHYAYA, *Linearizable eigenvector nonlinearities*, SIAM J. Matrix Anal. Appl., 43 (2022), pp. 764–786, <https://doi.org/10.1137/21M142931X>.
- [6] D. A. COX, J. B. LITTLE, AND D. O’SHEA, *Using Algebraic Geometry*, Grad. Texts in Math. 185, Springer, 2006.
- [7] D. A. COX, J. B. LITTLE, AND D. O’SHEA, *Ideals, Varieties, and Algorithms: An Introduction to Computational Algebraic Geometry and Commutative Algebra*, corrected 4th ed., Springer, Cham, 2018.
- [8] C. D’ANDREA AND G. JERONIMO, *Rational formulas for traces in zero-dimensional algebras*, Appl. Algebra Engrg. Comm. Comput., 19 (2008), pp. 495–508.
- [9] C. D’ANDREA, T. KRICK, AND M. SOMBRA, *Heights of varieties in multiprojective spaces and arithmetic Nullstellensätze*, Ann. Sci. Éc. Norm. Supér. (4), 46 (2013), pp. 549–627.
- [10] C. D’ANDREA AND M. SOMBRA, *A Poisson formula for the sparse resultant*, Proc. Lond. Math. Soc., 110 (2015), pp. 932–964.
- [11] C. EFFENBERGER AND D. KRESSNER, *Chebyshev interpolation for nonlinear eigenvalue problems*, BIT Numer. Math., 52 (2012), pp. 933–951.
- [12] I. Z. EMIRIS AND B. MOURRAIN, *Computer algebra methods for studying and computing molecular conformations*, Algorithmica, 25 (1999), pp. 372–402.
- [13] B. GAVIN, A. MIEDLAR, AND E. POLIZZI, *Feast eigensolver for nonlinear eigenvalue problems*, J. Comput. Sci., 27 (2018), pp. 107–117.
- [14] B. HUBER AND B. STURMFELS, *A polyhedral method for solving sparse polynomial systems*, Math. Comput., 64 (1995), pp. 1541–1555.
- [15] E. JARLEBRING, W. MICHIELS, AND K. MEERBERGEN, *A linear eigenvalue algorithm for the nonlinear eigenvalue problem*, Numer. Math., 122 (2012), pp. 169–195.
- [16] S. LANG, *Algebra*, Springer, New York, 2002.
- [17] A. J. SOMMESE AND C. W. WAMPLER, *The Numerical Solution of Systems of Polynomials Arising in Engineering and Science*, World Scientific, 2005.
- [18] B. STURMFELS, *On the Newton polytope of the resultant*, J. Algebraic Combin., 3 (1994), pp. 207–236.
- [19] S. TELEN, *Solving Systems of Polynomial Equations*, Ph.D. thesis, KU Leuven, Leuven, Belgium, 2020, retrieved from Lirias.
- [20] S. TELEN, M. VAN BAREL, AND J. VERSCHELDE, *A robust numerical path tracking algorithm for polynomial homotopy continuation*, SIAM J. Sci. Comput., 42 (2020), pp. A3610–A3637, <https://doi.org/10.1137/19M1288036>.
- [21] S. TIMME, *Mixed precision path tracking for polynomial homotopy continuation*, Adv. Comput. Math., 47 (2021), 75.
- [22] M. VAN BAREL AND P. KRAVANJA, *Nonlinear eigenvalue problems and contour integrals*, J. Comput. Appl. Math., 292 (2016), pp. 526–540.
- [23] R. VAN BEEUMEN, K. MEERBERGEN, AND W. MICHIELS, *Compact rational Krylov methods for nonlinear eigenvalue problems*, SIAM J. Matrix Anal. Appl., 36 (2015), pp. 820–838, <https://doi.org/10.1137/140976698>.
- [24] R. VAN BEEUMEN, W. MICHIELS, AND K. MEERBERGEN, *Linearization of Lagrange and Hermite interpolating matrix polynomials*, IMA J. Numer. Anal., 35 (2015), pp. 909–930.